UNIVERSIDADE

OF

BEIRA INTERIOR

DEPARTAMENTO DE CIÊNCIAS AEROESPACIAIS

DRAG REDUCTION OF AIRFRAME AND NON-LIFTING ROTATING SYSTEMS

Gonçalo Alexandre da Graça Pereira

DISSERTATION TO OBTAIN THE DEGREE OF MASTER IN AERONAUTICAL ENGINEERING

AUGUST 2009

Gonçalo Alexandre da Graça Pereira

DRAG REDUCTION OF AIRFRAME AND NON-LIFTING ROTATING SYSTEMS

Dissertation of Master in Aeronautical Engineering presented to the University of Beira Interior, 2009

Thesis developed under coordination of
Professor Eng. André Resende Rodrigues Silva

in association with:

To Rute

...for all the moments, inspiration and comprehension.

Abstract

Acting as a bridge for the development of the aeronautics sector in the European Union, the Clean Sky project is being developed in partnership with leading European manufacturers of aircraft and their components. Taking into account all the environmental problems addressed during the recent past, this project has the goal of revolutionizing the industry through the construction and operation of aircraft with a low environmental impact. Consequently, the development of this dissertation focuses on the Green Rotorcraft (GRC2) project that is part of the mentioned European programme, which aims to shorten the time to market for new solutions tested on heavy-sized utility aircraft, aerodynamically improved to reduce fuel consumption and consequent emissions.

The present work shows, through a literature search focused on guidelines and studies for active and passive control methodologies, a theoretical review of methods to reduce the parasite drag of the fuselage and non-lifting rotating systems with the objective to implement them on heavy-sized helicopters, which can ensure the achievement of the primary objectives established by the European Commission for the Clean Sky programme. Consequently, design guidelines are shown with practical examples demonstrated, to give evidence and enable the development of this project.

An analytical work is performed in this thesis, divided into two distinct areas: Active Horizontal Stabilizer, to trim the fuselage; and Cooling Systems, improved to reduce their net ram drag. Optimization solutions are presented in this research, showing the theoretical benefits obtained from the implementation of such changes.

Resumo

Actuando como ponte para o desenvolvimento do sector aeronáutico na União Europeia, o projecto Clean Sky está a ser desenvolvido em parceria com os principais construtores europeus de aeronaves e respectivos componentes. Tendo em consideração todos os problemas ambientais abordados nos últimos anos, este projecto tem como objectivo revolucionar a indústria aeronáutica através da construção e operação de aeronaves com reduzido impacto ambiental. Desta forma, o desenvolvimento desta dissertação incide sobre o projecto Green Rotorcraft (GRC2) que faz parte do programa europeu mencionado, visando à redução do tempo de construção de novos conceitos para uma aeronave da categoria Utilitário pesado melhorada aerodinamicamente de forma a reduzir o consumo de combustível e consequentes emissões poluentes.

O presente trabalho mostra, através de uma pesquisa bibliográfica focada em directrizes e estudos para métodos de controlo activo e passivo, uma revisão teórica de métodos para redução da resistência ao avanço parasita da fuselagem e de sistemas rotativos que não produzam sustentação com o objectivo de os implementar helicópteros pesados utilitários, assegurando assim o alcance dos principais objectivos estabelecidos pela Comissão Europeia para o programa Clean Sky. Assim sendo, são propostas directrizes de projecto com exemplos práticos demonstrados que comprovem e viabilizem o desenvolvimento deste projecto.

Nesta tese é realizado um estudo analítico, dividido em duas áreas distintas: Estabilizador Horizontal Activo, para trimar a fuselagem; e Sistemas de Arrefecimento, melhorados de forma a reduzirem a sua resistência ao avanço. Durante este estudo são apresentadas optimizações, mostrando os benefícios teóricos obtidos da implementação destes sistemas.

Acknowledgements

I would like to take this opportunity to express my thanks and appreciations to my academic coordinator, Professor André R. R. Silva, and to my industry coordinator, Nigel Scrase, for their advice and guidance during all the steps of this work as well as the constant availability through the development stage.

This work was made possible through the collaboration between University of Beira Interior, CEIIA and Agusta Westland.

I am grateful for all the support given from my colleagues at the Aerodynamics Department in Agusta Westland, with a special thanks to John Carmichael, Cristina Garcia, George Gardner, Edward Power and David Tring for all the assistance.

I would also like to thank to Jon Hamm, Mathew Horwood and Stephen Dymott for all the analytical research support.

I would like to extend a special acknowledgement to my girlfriend Rute and to my parents, for all the support and confidence throughout my academic path.

Gonçalo Pereira

Covilhã, 2009

Table of Contents

List of Acronyms and Abbreviations

EU	- European Union
JTI	- Joint Technology Initiative
ITD	- Integrated Technology Demonstrator
ACARE	- Advisory Council for Aeronautics Research in Europe
GTOW	- Gross Takeoff Weight
SFC	- Specific Fuel Consumption
ECS	- Environmental Control System
VG	- Vortex Generators
SJA	- Synthetic Jet Actuators
CFD	- Computational Fluid Dynamics
RANS	- Reynolds Average Navier-Stokes
EAP	- Electro Active Polymer
CG	- Centre of Gravity
SL	- Sea Level
OAT	- Outside Air Temperature
MGB	- Main Gearbox
IPCS	- Instrument Panel Cooling System
ACCS	- Avionics Cabinet Cooling System
MCSP	- Merlin Capability Sustainment Program
APU	- Auxiliary Power Unit
AW	- Agusta Westland

Nomenclature

f - flat-plate area

W_F - Weight of Fuel

δ - Pressure Ratio

θ - Temperature Ratio

C_{D0} - Drag coefficient based on frontal area

α - Fuselage Angle of Attack

D - Drag Force

q - Dynamic Pressure

D100 - Drag Force, in pounds, corrected to a speed of 100ft/sec at SL and Standard Conditions

List of Figures

[1] Figures taken from the official website of the project, www.cleansky.eu

[2] Figures taken from the website www,airliners.net

[3] Figure taken from the website commons.wikimedia.org/wiki/File:NOTAR_System.svg

[4] Figure provided by Agusta Westland

[5] Figures taken from the website www.flightglobal.com

List of Tables

Chapter 1

INTRODUCTION

1.1 Objectives

The purpose of this work is to give an overview through all the technology available nowadays that could help to get a solution for the last major problem faced by the Aeronautic Market, to bring the latest EU demands into reality. In this document, priority will be given to the reduction in airframe drag of medium to heavy-helicopters by gathering all the information available in literature cited. Continuing with this subject, various academic and industry methods are presented to improve the aerodynamic characteristics for the Rotorcrafts.

The next step is to make an analytical research of helicopter efficiency, divided into two main subjects. During the first study, consideration will be given to the possibility of implementing an Active Horizontal Stabilizer that can optimise the pitch attitude during forward flight. The second topic is to examine current diverse Cooling Systems implemented on heavy-sized helicopters with the objective of producing a theoretical way of making one global Cooling System that could improve the overall drag characteristics.

1.2 Clean Sky

Air Transport Systems, nowadays, are one of the most important elements for society, having a decisive role in making the world a global community through interaction of different cultures and promoting economic growth across the globe.

The Clean Sky project is a "Joint Technology Initiative" (JTI)[6] which will develop some new technology solutions to reduce the negative impact of the air transport on the environment. This is one of the largest European research projects to date, supported equally by the European Commission and Industry partners with a budget estimated at 1.6 billion Euros, where 160 million of them are intended to the rotorcraft Integrated Technology Demonstrator (ITD), managed over the period 2008-2015, representing 86 organizations and 16 countries. The concepts developed through this initiative will provide technological breakthrough developments and will frame them in market scenarios with solutions tested on Full Scale Demonstrators (established in 2013-14).

Therefore, Clean Sky JTI will try to implement new, radically greener Air Transport products that will:

- Provide a quick response to the Aeronautics Industry in the delivery of technology to markedly improve the environmental impact of the air quality;
- Improve the European Industry competitively, in order to contribute to the European Union objectives;
- Take leadership that serves to inspire the rest of the aviation world to provide greener products.

The next figure represents a diagram of what will be the framework schedule expected for the Clean Sky project, specifying the years with their respective task, giving an overall understanding of this initiative.

[6] "JTI is a type of project created by the European Commission for funding research in Europe to allow the implementation of ambitious and complex activities, including the validation of technologies at a high readiness level. The size and scale of JTI requires the mobilisation and management of very substantial public and private investment and human resources."

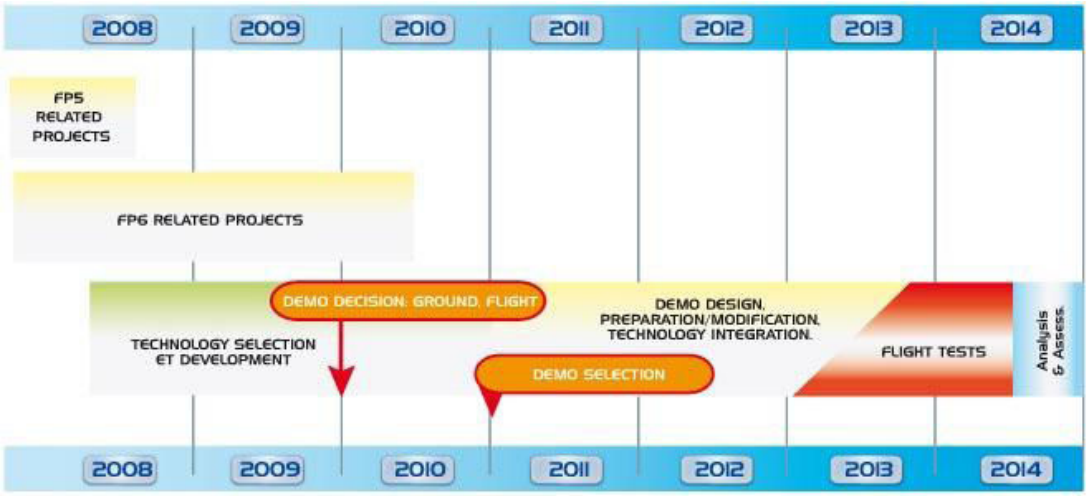

Figure 1.6. European Commission's Seventh Research Framework Programme

Content

This quick research process, offered by Clean Sky, represents an unprecedented opportunity for accelerated advance in the implementation of green technology in the Aircraft Industry.

During the time granted for this project, technology breakthroughs will be demonstrated and validated in order to make major steps towards the environmental sets by the Advisory Council for Aeronautics Research in Europe (ACARE) – the European Technology Platform for Aeronautics & Air Transport and to be achieved by 2020.

In the figure below are shown the three different goals sets by ACARE to improve the environmental aspect involved on this project, linked with each group of technology domain required to achieve the objectives.

Figure 1.7. Environmental goals sets by ACARE

The Clean Sky JTI is made up of six Integrated Technology Demonstrators (ITD):

- *SMART Fixed Wing Aircraft:* development of an active wing technology and a new aircraft configuration for breakthrough performance;
- *Green Regional Aircraft:* proposal for low-weight aircraft with smart structures, coupled with low external noise configuration, as well as the implementation of other ITDs technologies (such as engines, energy management and new system architectures);
- *Green Rotorcraft:* improvements around innovative rotor blades and engine installation for noise reduction, reduced airframe drag, integration of diesel engine technology and advanced electrical systems for elimination of noxious hydraulic fluids and fuel consumption reduction (which constitutes a teaming of Eurocopter/AgustaWestland leader initiative);
- *Sustainable and Green Engines:* produce five engine demonstrators to integrate technologies for low noise and lightweight low pressure systems, high efficiency, low NOx and low weight cores and novel configurations such as open rotors and intercoolers;
- *Systems for Green Operations:* attention made to all-electrical equipment and systems architecture, thermal management, capacity to accomplish "green"

trajectories/missions and improved ground operations to reach extensive benefits of Single European Sky;

- *Eco-Design:* focus on green design and production activities, withdrawal, and recycling of aircraft, through an optimized use of raw materials and energies thus improving the environmental impact of the whole products life cycle.

In figure 2.3 is possible to understand the working flow implemented for the interaction between the six independent ITD's and the simulation facility - Technology Evaluator.

Figure 1.8. Integrated Technology Demonstrator's

All of the developments will be assessed by the Technology Evaluator, which is a simulation facility that will assess the performance of the technologies following their review. This provides a process of looking at trade-offs, as some technologies may prove to have a more significant impact than others. The evaluation process will additionally enable the program to have coherent, unified and efficient development and structure.

Green Rotorcraft

Progressively, rotorcraft operations are growing to meet the demands of the European population. This effect can be seen in the following areas: medical service for safe and quick transport of patients and living organs for transplantation, passenger transport from city heliports to airports, and also between cities or areas where an efficient surface transport network cannot be developed for geographical or economical reasons.

The figure 1.4 outlines the goals to be achieved by the Green Rotorcraft ITD at the end of the Clean Sky project.

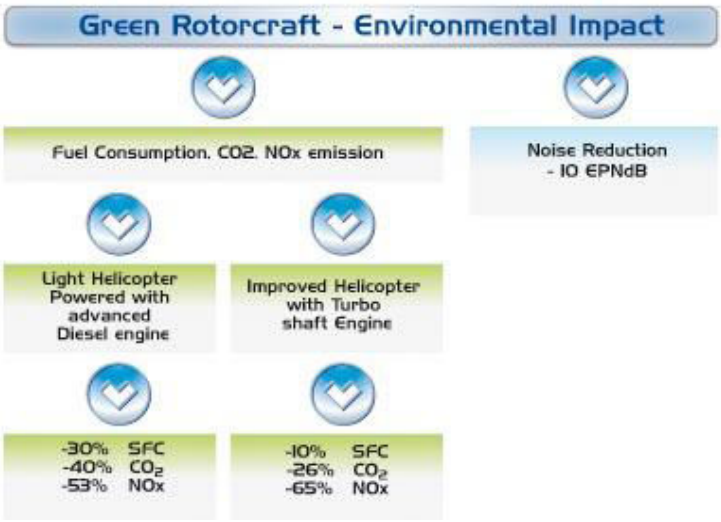

Figure 1.9. Areas of Technology Development for the Green Rotorcraft ITD

The Rotor blades designed or modified by the Green Rotorcraft initiative are expected to have enhanced capabilities by passive methods and active control techniques to reduce impulsive air loads and as a consequence, the radiated noise. At the same time, attention will be given to the turbo-shaft engine installation, improved with both the re-design of air intakes and exhaust nozzles to minimize the noise especially in hover and low speed flight conditions.

With the same weight of importance, “cleaner and more efficient power use” provides a need for development of aerodynamic subjects such as:

- Design of features on the airframe for the reduction of aerodynamic drag and download in cruise flight conditions;
- Engine integration through the adaptation of Diesel engine technology to light helicopters and turbo-shaft engine installation optimised for minimal power loss;
- Innovative electrical systems architectures enabling energy management optimisation on helicopters, implementing generic principles within the Eco-Design ITD.

1.3 Parasitic Power

One of the most important subjects related to helicopter performance is the parasitic power (or parasite drag). During the past years, a major effort has been taken to try to reduce this contribution for "dirty" designs. The parasitic power is known as a power loss generated from the viscous shear effects and flow separation on the airframe, tail, rotor hub, and various other sources on the aircraft frame/structural components. Through the overview of the next graph on Figure 1.5, this source of drag can be very significant as the helicopter advances at higher forward flight speeds, because helicopter airframes are much less aerodynamic than equivalent fixed-wing counterparts.

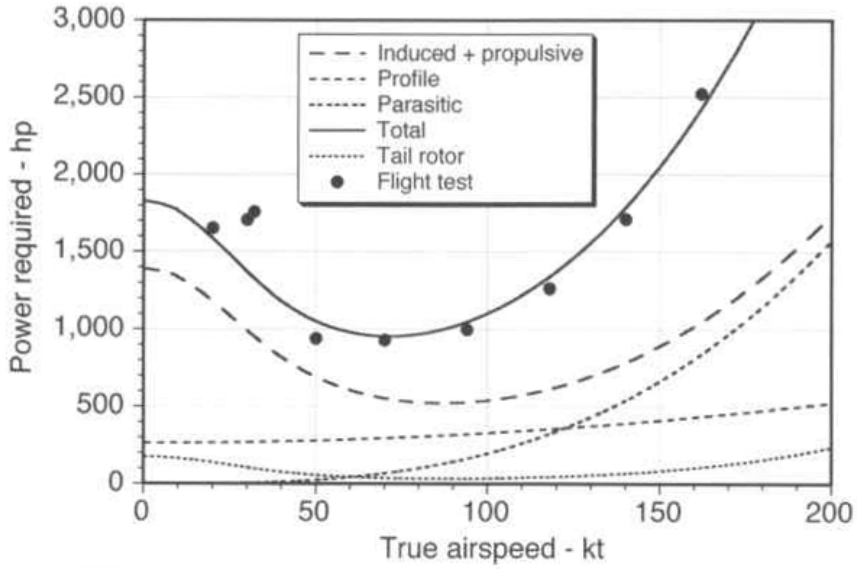

Figure 1.10. Predictions of main rotor power in forward flight (Ballin, 1987)

At the present time, it is usual to see values of *f* (equivalent wetted area or equivalent flat-plate area) - ranging from $10ft^2$ on light helicopters to $50ft^2$ on medium/heavy helicopter designs (Leishman, 2006 (1)).

The next figure illustrates the parasite drag portions produced by each component, or group of components, for current production configurations and for new designs.

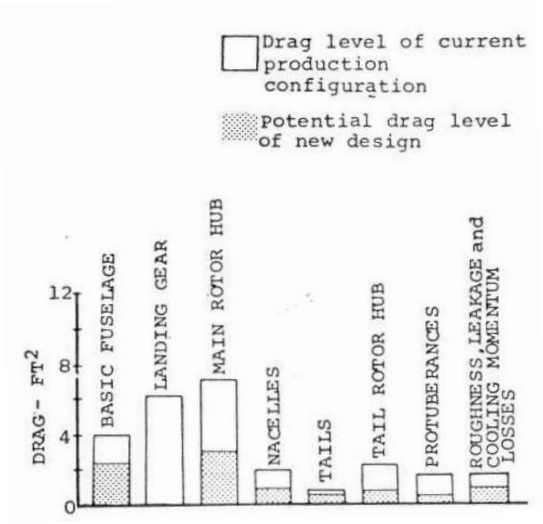

Figure 1.6. Parasite Drag breakdown for typical 20,000lb single rotor helicopter (Keys & Wiesner, 1975)

The power required in forward flight is also a function of helicopter weight. Normally, the final performance results are represented in terms of gross takeoff weight (GTOW) because the fraction of fuel carried, relative to gross weight, is very small. Thereby, the excess power available becomes progressively less with the increase of GTOW, and it's more perceptible at lower speeds where the induced power constitutes a larger portion of the total power.

1.4 Engine Installation

Within the helicopter industry, there are three different types of turbine engine installation. For the two first approaches, the engine is mounted either directly ahead or behind the main transmission, depending on if they are frontly or rearly driven

respectively; the engines could also be mounted on both sides of the transmission with the addition of angle drive gearboxes. For any of these configurations, there are advantages and disadvantages.

When the turbine engines are mounted forward or aft, an increase on the cross sectional area is avoided to accommodate them, but there are known complications with both inlets and exhausts. It is common to use simple pitot intakes on front mounted engines, but the exhausts end being directed sideways, which incurs an inherent moment drag; the rear mounted engines normally involve double bends in their inlet ducts with attendant power losses.

A different option is to have turbine engines mounted on both sides, which are preferable in terms of accessibility, balance and battle damage points of view. This type of engine configuration does not place any restrictions on the inlet or exhaust design; however this installation tends to increase frontal area and interference drag (particularly on the rotor hub).

Knowledge of the engine fuel burn is always required for an easy understanding of various performance problems, such as the range and endurance type of calculations. Engine performance data are usually expressed in terms of specific fuel consumption SFC (in units of lb/hp.hr or kg/kW.hr) versus shaft power (in units of hp or kW) as it can be seen on Figure 1.6 below.

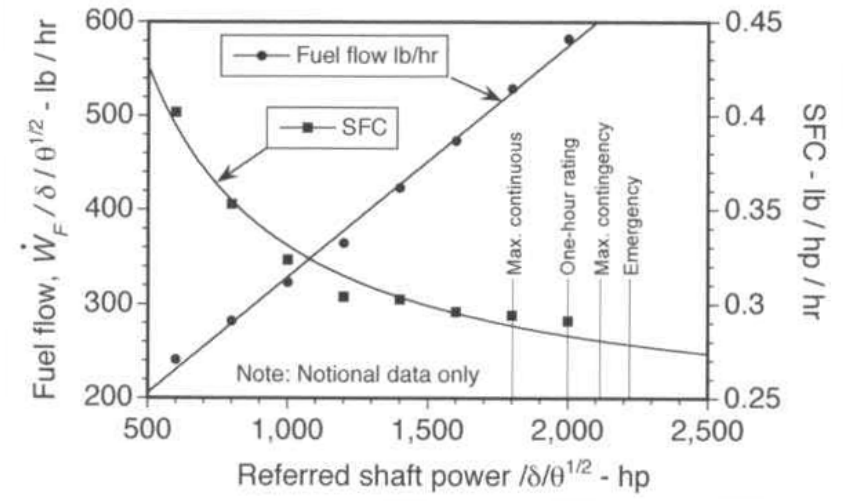

Figure 1.7. Normalized specific fuel consumption and fuel flow for a notional turbo-shaft engine (Leishman, 2006)

Chapter 2

LITERATURE SEARCH

2.1 Introduction

The current in-service helicopters hold parasite drag levels are far in excess of equivalent fixed wing aircraft. As shown by Keys & Wiesner (1975), a 20,000 lb helicopter would have approximately ten times the parasite drag of a turboprop airplane with the same gross weight, and at a speed of 150 knots this drag accounts for 45 percent of the total power required. Therefore the importance of reducing helicopter cruise power requirements is increasingly evident in light of the higher speed demanded of new helicopter designs and the current energy crisis (Leishman, 2006 (1)).

The graphic represented on figure 2.1 is a way of showing the benefits that can be reached in terms of drag through a proper guideline for drag reduction on future production helicopters.

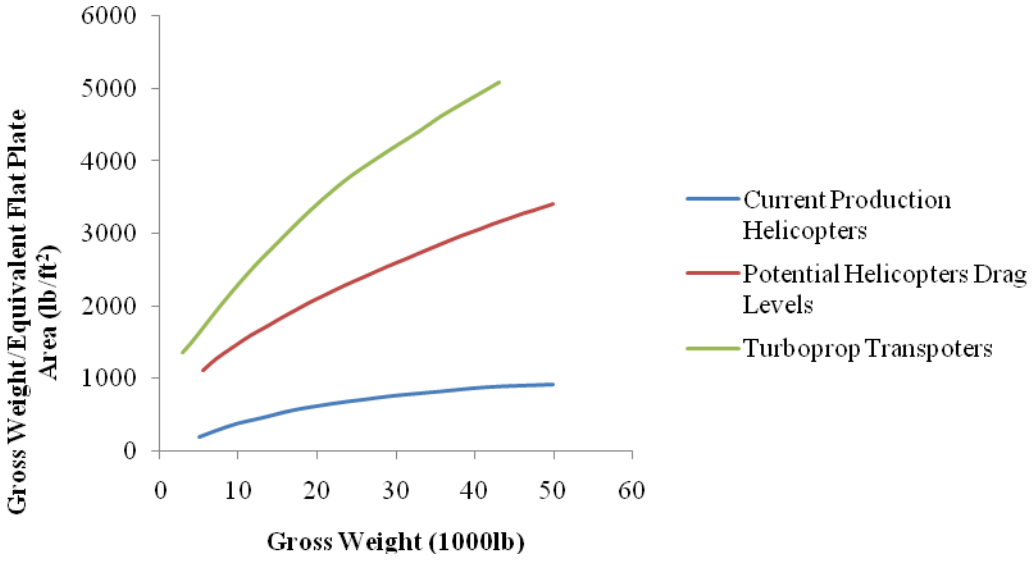

Figure 2.1. Helicopter/fixed-wing aircraft drag trends (Keys & Wiesner, 1975)

Regarding an actual vehicle design, there are many varied design requirements with associated geometric constraints which may adversely affect the drag. In most cases they are not entirely rigid and may be traded off to a certain extent with the generally conflicting criteria for low drag. Unfortunately, this trade-off may be very difficult to quantify in terms of the estimated drag reduction with its anticipated benefits versus the possible penalties. The capability to adequately examine and quantify the effect of a design change becomes available to the industry through improved mathematical modelling techniques (Williams & Montana, 1975). There are available data on helicopter parasite drag reduction but relatively little flight test data. Although the tunnel data drag reduction experiences already made rarely progresses to production mainly because the customer does not set a very high priority on low drag in his specification (Gatard et al, 1997).

It is widely known that the fuselage is the largest airframe component on a helicopter (although if well designed can have relatively low drag), so its aerodynamic characteristics can have a significant impact on the performance of the helicopter as a whole. Practical constraints, such as the need for rear loading doors, means that the shapes that are typical of helicopter fuselage designs often tends to flow separation and high drag. In addition, the airframe often operates in the main rotor wake, which changes the aerodynamic characteristics compared to those obtained without the rotor (Wilson & Ahmed, 1991).

Table 2.1. Drag audit of an hypothetical, recently designed, heavy-sized helicopter

ITEM	Drag Portion (%)
Basic Fuselage	18,59
Cowls	11,19
Hub	17,72
Stubs	5,51
Shanks	3,44
Blade Roots	1,72
Rotational Effect	2,58
Sponsons	5,34
Empennage	6,88
Tail Rotor Head	5,16
Cooling	5,86
Engine Drag	-0,34
Aerials & Excrescences	16,01
Flotation	0,34

Through the overview of the drag audit presented on the table above, on recent production medium to heavy-sized helicopters, it is usual to find fuselage parasite drag values, with all of the components fitted, accounting for 60-70% of the total parasite drag.

A prospective improvement in helicopter capability due to a decrease in drag and a consequent increase in efficiency appears to be very substantial. In addition to the more obvious aspects of increased range, payload, and maximum speed, there are several additional payoffs which are not as apparent. One of these is the reduction in aircraft size and gross weight needed to perform a given one mission. An increase in efficiency due to a reduction in drag produces an associated reduction in power required which in turn reduces engine/drive system size and results in reduced weight. The reduced size and weight further reduces power required, and so on until the design process converges. This multiplicative effect is only possible if a drag reduction is introduced in the early design stages – before the aircraft configuration is frozen (Gormont, 1975); (Hermans et al, 1997).

The consequence of a considerable reduction in parasite drag must be assessed from the point of view of the entire aircraft system. The possible benefits are strongly dependent on the particular helicopter mission/role; for instance, each of the five primary "performance missions" – range, payload, speed, endurance and hover have somewhat separate implications for drag. Adding the performance aspects, there are numerous operational requirements which should also be assessed in terms of drag. Each of these is amenable to design compromise so that the aerodynamic drag can be minimized while still permitting maximum operational effectiveness.

Another critically important factor is the cost trade-off – design / development / production / maintenance and operational costs (which include both direct fuel and fuel logistics costs). It can be demonstrated that, for many missions, it is entirely possible to develop smaller, lighter and cheaper aircrafts by designing for low drag; however, this only happens if a low drag philosophy is implemented in the initial design stage (Duhon, 1975).

One aerodynamicist is always trying to find ways to reduce drag, but his ideas usually cost money and weight. Therefore he has to sell his ideas to the weight and cost people. Any effort to reduce helicopter parasite drag must be evaluated in terms of its

effect on the helicopter's weight, cost to manufacture, and cost to operate. Two factors in the current environment – Design to Cost and the soaring price of fuel – make it more important than ever to look carefully at the value of a particular drag reduction approach. Design to Cost is a factor not only in military procurement, but is also deeply involved in the competitive field of commercial helicopter sales. Therefore any added cost attributed to drag reduction must balance favourably against the overall benefits it brings. Fuel costs, which used to be almost negligible in the total cost of owning and operating a helicopter, are now quite significant, and thus emphasis are added on improving cruise efficiency. Undoubtedly now, more than ever before, the stage is set for a vigorous attack on parasite drag reduction (Stroub & Rabbot Jr., 1975); (Wiesner, 1977).

The most important effect of drag on rotorcraft flight, of course, relates to vehicle performance. Although efforts to minimize drag are directed substantially toward maximizing speed and fuel economy, it is worthwhile, and often essential, to consider the relationship between drag and flight dynamics characteristics.

Given that drag reduction procedure impacts aircraft stability, variations in the vehicle design will probably be indicated to correct the stability modification. Design variations like this should be anticipated so their cost, weight, and other factors can be considered in assessing the merit of the drag reduction procedure.

As soon as analysis and test programs are instigated for the study and improvement of the rotorcraft drag problem, the activities should be conducted to gather the most useful technical information for the cost. For that reason, when an analysis or test is designed specifically to consider drag issues, minimal additional effort would yield extremely useful stability information. Measuring fuselage stability derivatives as part of a drag measurement wind-tunnel test is a good example. In order to carry the stability and control aspects of drag reduction along the projected course, it is first necessary to identify connections between the problems (Hoffman, 1975); (Gleize et al, 2001).

2.2 Sources of Performance Loss

2.2.1 Fuselage

Beginning with the Nose Section, the major problem is concerning to the corner radii adopted to any model, in order to achieve a low drag nose shape. Therefore, every time the corner radius to fuselage width ratios reaches values below 0.1, there will be a noticeable increase in drag. In the other way, the Nose Section is relatively insensitive to contour (symmetrical/asymmetrical) from a drag point a view.

In the Cabin Section, when the aircraft flies with negative incidence, the drag rise of a square section is four times greater than a circular. Simultaneously with this, windows and doors located at the Cabin Section can produce drag by themselves if they are not flush with the surface contours.

The chart in the next figure shows two principal theoretical cross-sections with the intention of comparing it with a typical helicopter fuselage shape.

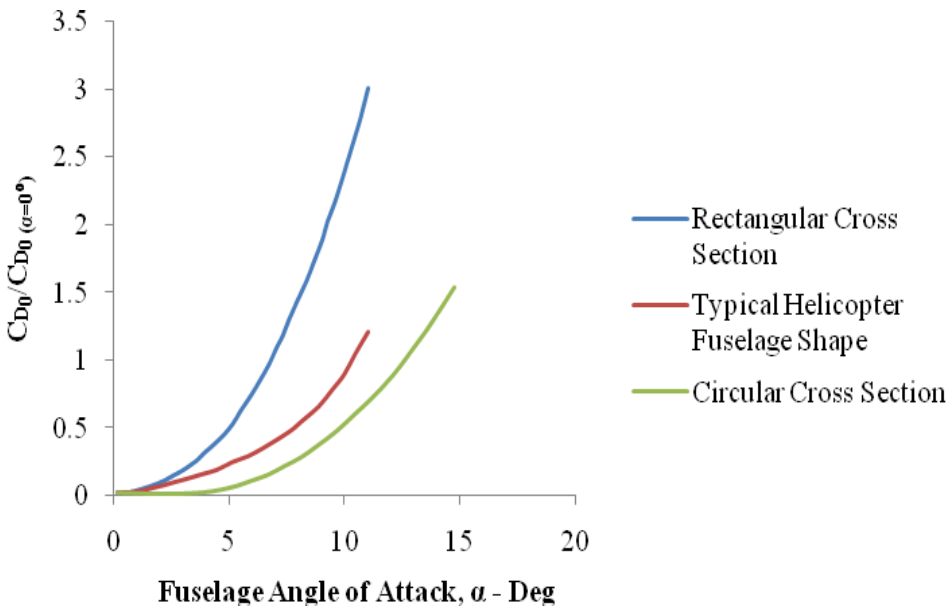

Figure 2.2. Effect of fuselage cross-section shape on drag (Keys & Wiesner, 1975)

One of the most critical sections of helicopters is the After-Body. This region represents the largest drag contributing area of the airframe. Supporting this, if a contraction ratio (l/D - contraction length/equivalent cabin diameter) below 2.0 is reached, will be present a flow separation increasing the after-body pressure drag. Another important design issue to look here is the negative after-body camber (which shifts the fuselage zero angle of attack) and the minimum drag point angle for cruise conditions, because this has a tendency to increase the drag and cruise download (Clar & Wilson, 1980); (Polz & Quentin, 1981); (Seddon, 1982); (Epstein et al, 1994).

Regarding to the overall airframe, any sudden changes in curvature such as rivets or sharp edges around doors are likely to increase parasite drag values due to unnecessary flow separation. Apart from this, all the leakages such as holes and recesses or large size and number of bluff-body surfaces, like fairing designs, will be penalized with a drag increment (Gaudet, 1987).

Another usual source of parasite drag is the Cowls. As these are additional items added to the basic fuselage, they create drag by the increment of the frontal area and change of profile. One common reason for this implementation is for stability purposes, but the main drawback to a full fairing is the increase in mass, along with the complexity of access (growing maintenance time to remove/refit fairings and thus costs). But on the other hand, we can find a high base drag on side mounted engine cowls that could be responsible for almost 50% of general cowling drag.

One of the last design improvements achieved in the wake around the hub is the pylon fairing, which is closely linked to the aerodynamics of the rotor head. Implementing this pylon geometry in the aircraft, the interference drag between hub and fuselage is decreased, but the frontal area of this fairing creates drag by itself (maximizing the adverse pressure gradient when the pylon largest frontal area is before of the rotor hub.

Parallel with the overall design of the airframe, the landing gear is an important item when the parasite drag subject is approached. When the option of implementing a skid gear is taken, additional drag will be added because of the increment on frontal area. Still, the use of this concept is 40% lower in drag than fixed wheeled gear (Harrington, 1954).

A common decision adopted on the latest heavy-sized helicopters is the use of sponsons. But as this item can be seen as a protuberance, it reduces the aerodynamic

efficiency of the fuselage adding weight and drag to the airframe. When this component lacks aerodynamic design, large drag penalties will be added to the airframe.

With the same importance, the empennage is another vital design item that needs extremely care. So, the effectiveness of a lifting surface here, such as a fin or a tail plane, can suffer as a result of a gap between the surface and the fuselage or a cut-out in the leading edge. Such is the case when providing ventilation for an intermediate gearbox. Together, where a tail plane or a tail rotor gearbox fairing is located on the fin, particularly if there is an interference with the leading edge, there is a danger of flow breakdown which can reduce fin effectiveness and create excessive drag. Finally, a less careful shape design in the horizontal stabilizer and the vertical fin will increase normal tail download condition and tail rotor fin drag, respectively.

2.2.2 Protuberances

The main problem of this group of items is the quantity that can be found on any modern helicopter, reaching a considerable percentage of parasite drag.

Aerials have a negligible effect on drag individually, but can be significant due to the numerous amounts of them on aircraft. As they, normally, are not taken into account to be aerodynamically efficient, a bad positioning of externally mounted antennas could result in a considerable increment to parasite drag (Lowson, 1980).

This graph presented on figure 2.3 demonstrates the influence of aerials (Antenna) on the helicopter drag, giving the example of two different sections.

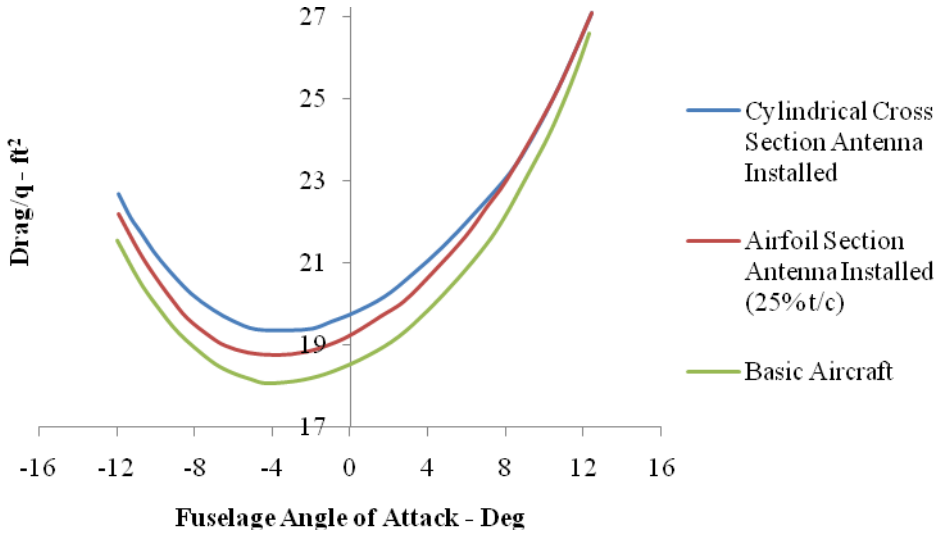

Figure 2.3. Effect of streamlining on antenna drag (Keys & Wiesner, 1975)

As an optional item for helicopters, the radome is one of the most problematic issues in relation to drag. The main factors affecting radome drag are: a) radome diameter, b) radome depth, c) radome location (aft of nose), d) lower edge radius, e) presence or otherwise of splitter. The factors (a) and (b) are governed by the radome size requirements and little can be done to influence the dimensions. The radome location is usually dictated by practical (structural) considerations but does have a small effect on drag. A radome can cause stability problems by vortex shedding especially when placed under the nose.

In the excrescences, any external component that is not retractable or flush with the fuselage will add drag penalties to the project as with careless undercarriage doors design. For the components located on the exterior of the aircraft that shows considerable frontal area and hence the drag area, as well as incorrect positioning, will create instabilities in the design and therefore increasing drag. The airflow over the fuselage varies considerably in speed from one location to another. The same item fitted in a region of high speed flow will create far more drag than if it were fitted in a region of slow moving air (Greenwell, 1997).

When one helicopter model is designed for Navy roles, it is common to incorporate a flotation system. Normally this system is divided in four inflatable bags,

two on both aft sides and another two on either sides of the nose. Therefore, when these components are not fitted flush on the airframe, they increase the pressure drag. In external applications, there will be drag penalties for the changed structural design shapes.

2.2.3 Cooling Systems

One of the most important matters for all the mechanical and electronic components in the aircraft is the cooling systems. Environmental Control Systems (ECS) of the aircraft require ducts to drain the air, which will tend cause spillage and ram drag, and at the same time there is potential for drag to be caused by the exhaust system of the cooling but the effect will vary based on the direction of the outlet. One of the best examples to verify this effect is on the cooling intake and exhaust areas for the intermediate and tail rotor gearbox mounted on the empennage, where excessive intake areas will penalize the design with excessive spillage and ram drag.

2.2.4 Engine Installation Performance

It is well known that the engine installation on helicopters is a very sensitive method, where any decision has pros and cons. Depending on size and number of engines that one model can include, there are various different configurations that can be adopted on the upper surface of the airframe, but parasite drag will be increased for any of those configurations at least by bigger frontal area influence. Location is also important to obtain sufficient flow and avoid the ingestion of hot air from exhausts or cooling outlets, therefore increasing the power losses (Perry, 1979).

The performance around engine installations on helicopters airframe generally results in deteriorated properties when compared to the engine manufacturer's performance specifications. It is normally settled that the engine installation losses can be divided into inlet losses, exhaust losses, and losses due to bleed air extraction (Stepniewski & Keys, 1984). A succinct discussion of each of these three subjects is presented next:

- Inlet losses usually occur with either a rise in temperature or a pressure drop at the inlet. During hover flight, the principal effect is the temperature rise due to the recirculation of hot exhaust gases which happens mainly in ground effect. It is also seen that, for installations with the gearbox located in front of the inlet, a noticeable rise in inlet air temperature can be identified. Pressure losses generally result from flow disturbances or separation at, or ahead of, the inlet; this is especially noticed in forward flight, where flow separation may end in sizeable pressure losses; however, these losses are often offset by a decrease in flow velocity and an increase in air pressure as it enters the inlet (ram recovery). When particle separators or screens are installed, additional considerable losses may occur both in hover and forward flight.
- Exhaust losses are commonly caused by backpressure normally resulting from a redirection or rerouting of the exhaust air flow, from the installation of equipment such as an infrared suppressor, or from nozzeling to reduce parasite drag.
- Extra losses are added to the installation if bleed air is extracted from compressor for anti-ice protection of the engine inlets when operating under cold ambient temperatures or for cabin or cockpit air-conditioning systems under hot ambient conditions.

The engine installation losses are minimized for designs having podded engines because the engines are essentially detached from the airframe. With flight test data experiences, the power losses for this type of installation are generally less than one percent. Consequently, the one-percent loss assumed that there is no increase in the power available due to ram recovery effects in forward flight.

The presumably loss of power due to the inlet pressure drop (as a result of engine installation) also leads to a consequent decrease in fuel flow. Typically, a loss in pressure will result in a reduction in fuel flow of 0.5 percent or less for each one-percent decrease in power available, thus resulting in a net increase in SFC. On the other side, a temperature rise will produce approximately equal power and fuel flow reductions without any net SFC change.

2.3 Performance Improvements Methods

2.3.1 Passive Drag Reductions

2.3.1.1 Design Aspects

In order to achieve an optimal airframe concept, there are several practical design guidelines to follow so the helicopter can be as efficient as all the means available nowadays allows it to be. Therefore, will be presented next a group of particularities that can make the difference on the design:

- The corner radii of the nose shape should be kept with corner radius to fuselage width ratio below 0.1 in order to avoid drag increments;
- It is preferable to use a cabin cross-section almost circular, so the drag rise can be minimized when the aircraft face negative fuselage incidences;
- Windows and doors should be flush with the surface contours and door tracks recessed to reduce the flow discontinuities along the fuselage;
- Make a carefully tapering of the after body lines gradually to avoid flow separation, contraction ratio of at least 2.0 is required to obtain minimum after-body pressure drag;
- Effort should be made to avoid negative after-body camber (shifts the fuselage zero angle of attack) and the minimum drag point to more positive angles because it tends to increase the drag and download on cruise conditions;
- Any sudden changes in curvature such as rivets, or sharp edges around doors, should be implemented as flush as possible;
- Attention should be given to leakages such as holes and recesses, size and number of bluff body surfaces and fairing designs of high frontal area;
- In terms of airframe aerodynamics, ideally, the landing gear should be implemented as retractable with flush covering doors so no drag can be associated to it;
- Inverse cambered horizontal stabilizer and a cambered vertical fin to minimize drag of the normal tail download condition and the tail rotor fin combination, respectively, in cruise flight;

- Try to fit in some aerials embedded in the tail plane or even change their cross section would reduce their aerodynamic impact;
- The use of fairings and selective positioning can result in a sizeable drag reduction on protuberances because for components located on the exterior of the aircraft it is good practice to minimise the frontal area and hence the drag area, and it is also a good idea to place components behind one another so that the latter excrescence is in the wake of the preceding;
- Any component that is external to the fuselage should ideally be retractable into the fuselage, the undercarriage should be retractable as well and should be used undercarriage doors to minimize drag even further;
- The Flotation System should be as flush as possible through the fuselage in order to don't produce pressure drag;
- The inclusion of a splitter, located behind the radome, reduces drag and gives better, steadier flow behind the radome.

2.3.1.2 Spoiler

As an additional item (excrescence), the Spoiler is a device mainly used for stability purposes, deflecting the turbulent fuselage wake away from the tail plane increasing their directional stability and consequent effectiveness. Another consequence obtained from it, is a positive camber effect that can be beneficial for drag. Normally this device is located at the after-body region, where upsweeping is due to start. Because of the added lifting effect of the spoiler at cruise speeds, this creates nose down moments which, unless another devices are added to counteracts, could lead to an undesirable effect.

The next figure represents the aerodynamic study made on the spoiler implementation for the BO-105, in terms of drag and lift.

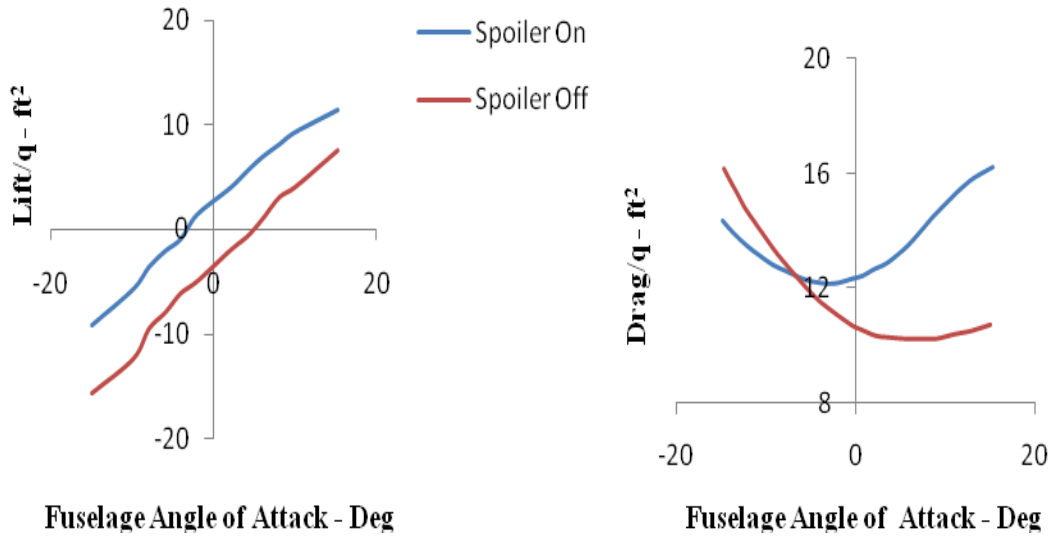

Figure 2.4. Effect of BO-105 spoiler on lift and drag during cruise flight (Keys & Wiesner, 1975)

While negative camber provides an unfavourable increase in drag, positive camber can be employed to shift the drag bucket to a desired nose down cruise angle of attack. An industry example is the spoiler installation on the BO-105, which was designed to deflect the turbulent fuselage wake and trailing vortices away from the tail rotor, thereby improving directional stability. This installation consists of a 2 ft^2 flat plate mounted on the lower portion of the fuselage. As shown in the following Figure x, the positive camber effect caused by this installation reduced the fuselage drag by an amount equal to the pressure drag of the spoiler, and resulted in no drag penalty at the -7^o cruise angle of attack.

The image shown on figure 2.5 is the rear view of the BO-105 where is possible to notice the yellow spoiler device, implemented on the upsweep.

Figure 2.5. MBB BO-105 with a spoiler device implemented

2.3.1.3 Strake/Deflector

There are two additional techniques to reduce the drag of cambered rear loading after-bodies, which are the installation of strakes and the use of deflectors.

Strakes have the purpose to reduce drag by forcing the two fuselage vortices formed by the intersection of air from the side and bottom of the after-body off the surface and downstream. The suction created by vortices is reduced by displacing them from the surface. Drag reductions associated with strake installations were verified during wind tunnel tests of a CH-46 and a Belfast CMK1. As can be seen in Figure x, presented on a research work made by Boeing Vertol Company*, the implementation of Strakes provide approximately 8% of drag reduction to the basic fuselage, and at the same time gives also an improvement in directional stability (Keys & Wiesner, 1975).

The next figure shows the benefits taken from the implementation of strakes on heavy-sized helicopters (CH-46), in order to reduce the fuselage parasite drag.

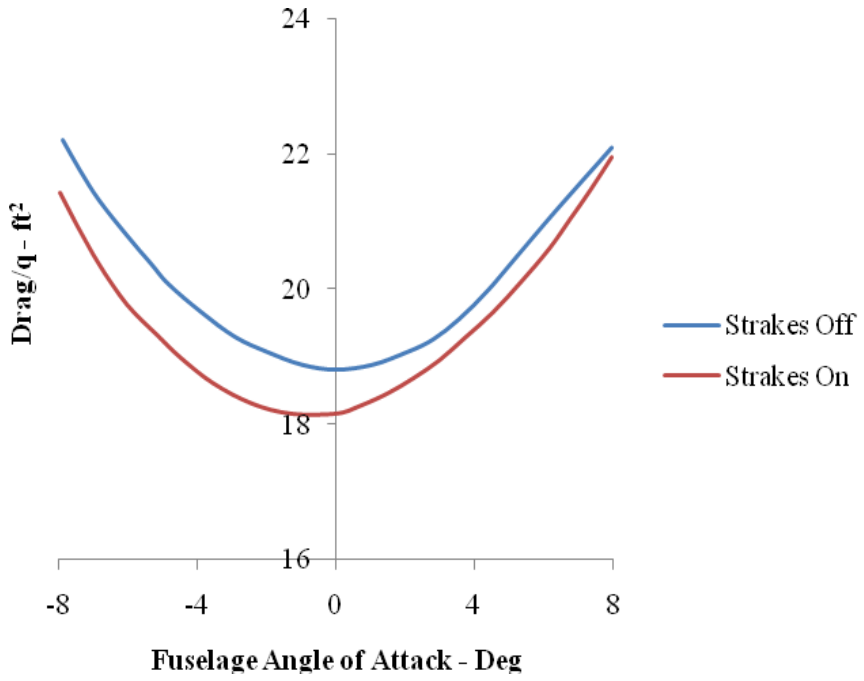

Figure 2.6. Effect of Strakes on the CH-46 helicopter fuselage drag (Keys & Wiesner, 1975)

Another interesting study is the one developed by John Seddon. This work performed and investigation into strakes on a Lynx fuselage and concluded that the results were unimpressive. However, with the use of deflectors, the results were much better and the experiment revealed that there was no change between vortex and eddy flow causing a larger drag. These deflectors are of small profile and likely to be of reduced mass. The increase in drag shown in the figure below for the results without the deflectors is due to the change in flow type, which with deflectors can be seen that the change in flow type, between vortex and eddy flow, does not occur (Seddon, 1983).

In the figure below can be seen a chart obtained by an aerodynamic analysis performed in order to understand the benefits taken from the use of deflectors on helicopters upsweep.

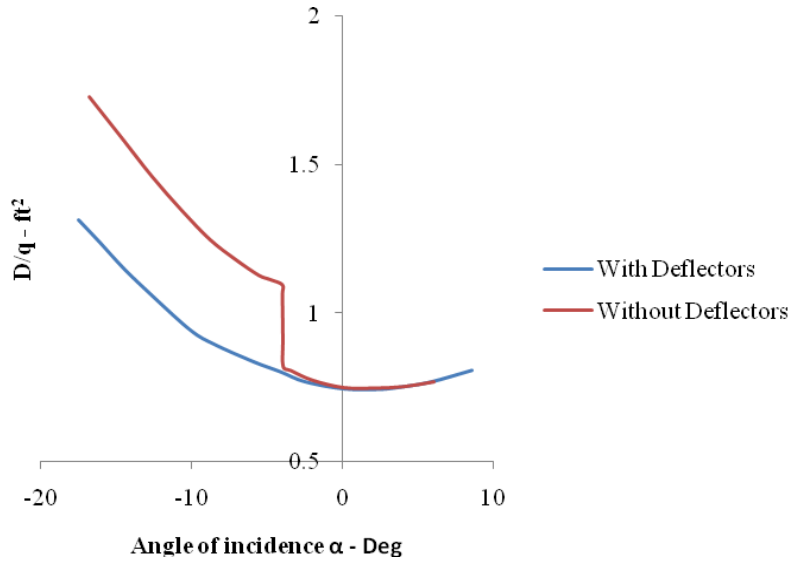

Figure 2.7. Effect of deflectors on helicopters upsweep (Seddon, 1983)

2.3.1.4 Vortex Generators

In this section will be presented a research on aerodynamic drag reduction, made by Mitsubishi Motors, to a roof end in a sedan vehicle and then easily adapted to the helicopter example.

Since the aircraft height to the lower region of the aircraft, in the after-body section, becomes progressively higher as the flow moves upstream, an expanded airflow is formed here. This causes the upstream pressure to low, which in turn creates reverse force acting against the main flow and generates reverse flow at upstream point C. No reverse flow occurs at point A located further downstream of point C because the momentum of the boundary layer is prevailing over the pressure gradient (dp/dx). Between points A and C, there is separation point B, where the pressure gradient and the momentum of the boundary layer are balanced. As shown in Figure x, in the lower zone close to the aircraft's surface within the boundary layer, the airflow quickly loses momentum as it moves upstream due to the viscosity of air. The purpose of adding VGs is to supply the momentum from the lower region where as large momentum to higher region where has small momentum by stream wise vortices generated from VGs located just before the separation point, as shown in Figure x. This allows the separation point to shift further upstream. Shifting the separation point upstream enables the expanded

airflow to persist proportionately longer, the flow velocity at the separation to become slower, and consequently the static pressure to become higher. The static pressure at the separation point governs over all pressures in the entire flow separation region. It works to reduce drag by increasing the back pressure. Shifting the separation point upstream, therefore, provides dual advantages in drag reduction: one is to narrow the separation region in which low pressure constitutes the cause of drag; another is to raise the pressure of the pressure of the flow separation region. A combination of these two effects reduces the drag acting on the aircrafts (Koike et al, 2004).

The next figure schematizes the boundary layer behaviour at a body upsweep and then shows the effect of the streamwise vortex generated by the VG.

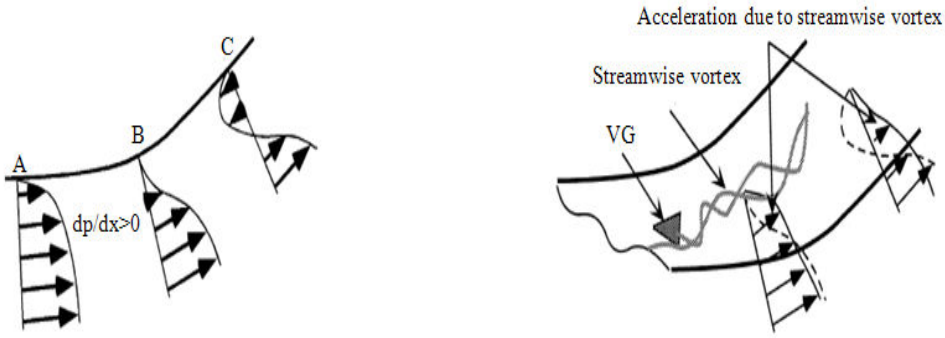

Figure 2.8. Schematics of velocity profile and flow around VG at the fuselage upsweep

However, the VGs that are installed for generating streamwise vortices bring drag by themselves. The actual effectiveness of installing VGs is therefore deduced by subtracting the amount of drag reduction that is yielded by shifting the separation point downstream. Larger-sized VGs increase both the effect of delaying the flow separation and the drag by itself. The effect of delaying the flow separation point however, saturates at a certain level, which suggests that there must be an optimum size for VGs.

Within this area, there are various shapes that can be implemented as VGs. But it is normal to found two main usual shapes: delta-wing and bump shaped. For the literature used in this report, we can assume that the delta-wing shaped VGs are the more effective, and it can be explained as follows: delta-wing-shaped VGs have a smaller frontal projection area, which means that they themselves create smaller drag.

Moreover, the vortex generated at the edge of a delta-wing-shaped VG keeps its strength in the flow upstream of the edge since it barely interferes with the VG itself because of the VG's platy form. With the bump shaped VGs, on the other hand, the vortex is generated at a point close to the upstream edge of the bump, which causes the vortex to interfere with the bump and lose its strength.

2.3.2 Active Drag Reductions

2.3.2.1 Synthetic Jet Actuators

Currently, it is easy to find helicopters that are designed for specific mission profiles but not purely optimised for aerodynamic efficiency. For instance, helicopters that have utility ramps usually have an upsweep at the rear of the fuselage limiting how streamlined the helicopter could be. Synthetic jet actuators located on the rear of the fuselage, for example, could be used to improve the airflow around the upsweep. The SJA's control the flow by taking in air of low momentum and ejecting it at high momentum thus accelerating the transition from laminar to turbulent flow, the advantage of these devices is that they require no extra plumbing to supply the air as the actuator sucks in the fluid itself, however power will have to be supplied to the device (Hassan et al, 1998); (Ben-Hamou et al, 2007). The diagram below is a representation of a typical SJA; however they can vary in size and geometry.

The figure below exemplifies the diagram of a zero-mass (theoretical) synthetic jet actuator with its resultant mode of operation.

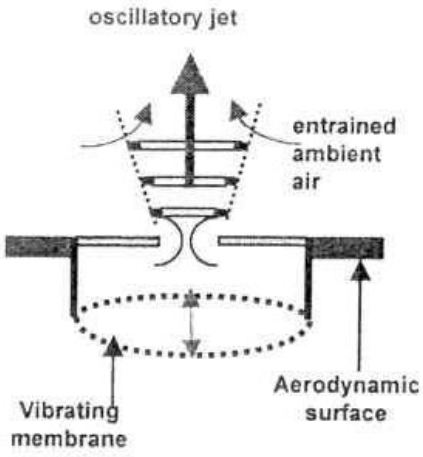

Figure 2.9. "Diagram Sketch" of a zero-mass synthetic jet actuator (Hassan et al, 1998)

A research paper by Boeing looked into the application of these actuators on a helicopter fuselage with the objective of reducing both the aft fuselage cruise download and drag. Boeing tested these actuators by placing 12 horizontal and vertical slots on the rear of the fuselage.

The figure 2.10 shows the rear view of the US Army/Boeing MDX wind tunnel model where can be seen the synthetic jet actuators configuration adopted on the rear fuselage upsweep.

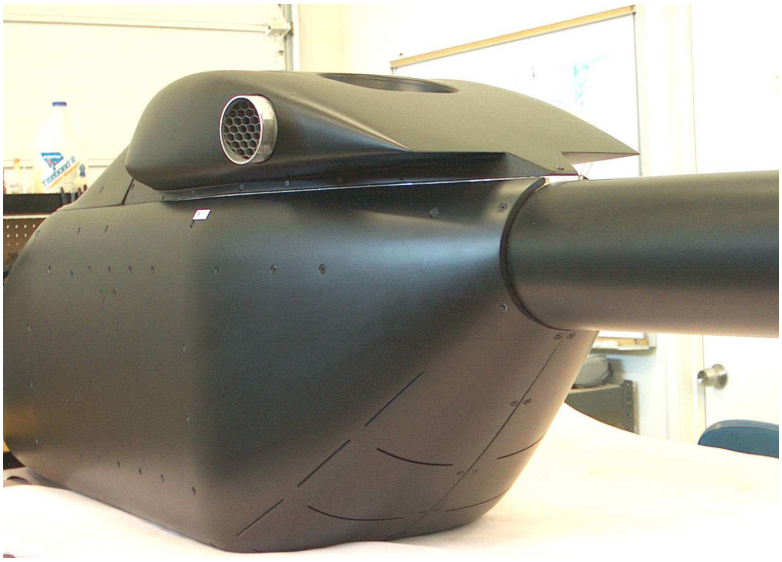

Figure 2.10. US Army/Boeing MDX Active Flow Control wind tunnel model showing jet slot configuration (Martin et al, 2005)

The Boeing used the idea that a number of SJA's can be operated collectively or independently to control the natural flow separation and reduce the drag caused by the after-body upsweep. The speed of the flow and the number of active slots would be controlled by a computerized system based on a function of flight conditions the helicopter is experiencing at that time.

Wind tunnel results found up to 10% drag reduction and 40% reduction in cruise download, which Boeing state outweighs the additional components required for SJA's, this percentage value is related to the baseline drag coefficient for the fuselage and hub including interference. However work needs to be done on scaling this to a full size helicopter, as an investigation would need to look into suitable actuators and location configurations could be less optimal than others. Utilising the full potential of SJA's would therefore require both a lot of wind tunnel and the use of CFD testing for different fuselage configurations, a badly configured system, could potentially result in undesirable performance characteristics and provide a detrimental effect due to the added mass of the system. This testing would likely be costly and has perhaps prevented previous attempts to look into the problem. Advanced CFD methods such as RANS solutions, are going some way to making the use of CFD a viable option, however this would require a good level of confidence in the output of the CFD before it can reduce significantly the amount of wind tunnel testing, which would require a thorough validation of the technique (Martin et al, 2005).

For commercial impact understanding, the University of Manchester performed an investigation into optimizing the scaling of the system for an Airbus aircraft for use with increasing maximum lift. Their conclusions found that, over the ¼ chord flap, the weight of the actuators was 34kg and power generation produced an effective 6kg, with other components creating a total of 50kg. It should be noted however that a helicopter would be much smaller than the Airbus, therefore the area that SJA's are placed on the helicopter would likely be less than the Airbus, actuation velocity will also likely be less (0.3 mach tested by Boeing is roughly 100m/s), therefore the power required and additional mass will likely be much less than the Airbus. Their SJA's, at the optimal 70m/s, were shown to produce 15% efficiency with 1.08W electricity to 0.168W mean

fluid power at 2.5Khz of frequency (maximum 130m/s 3W power, produced 7% efficiency) (Gomes et al, 2006).

2.3.2.2 Active Dimples

Recently presented on an Imperial College paper, this topic looked into the use of active dimples through electro active polymers, with the eventual idea of using it in airframe structures. The basic principle of electro-active polymers is that they can produce immediate vortex generator's, by the use of controlled circular diaphragm on the surface of the polymer that displaces downwards upon activation. This leads to a reduction in the skin friction, by injecting high momentum fluid into the lower part of the boundary layer.

The image represented in the figure below is a scheme that shows the principle of actuation of a dimple.

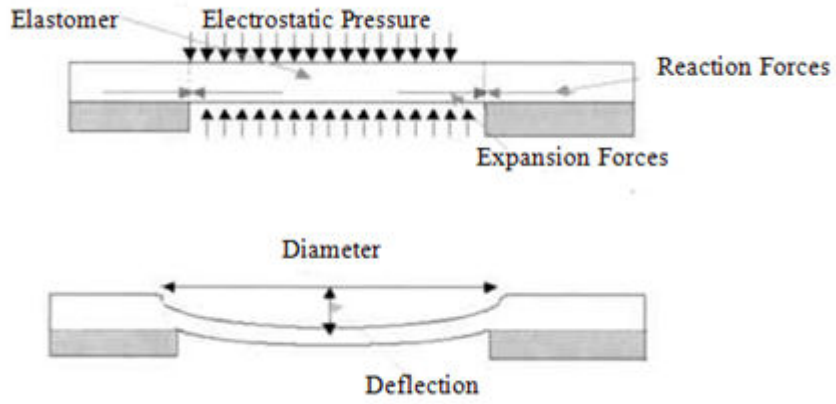

Figure 2.11. Principle of actuation of a dimple (Dearing et al, 2007)

This technology can therefore be used to control the flow separation experienced with bluff body's (rear upsweep as an example) by manipulation of the critical Reynolds number. Due to the system being active, the height of the EAP's can be altered therefore controlling the point where flow separation occurs. This can then produce a single vortex of known strength for a required amount of time. As the skin

friction is sensitive to the height of the dimple, an active system would need to be employed. Another reason for an active system is that it is stated within the paper, that dimples are most efficient in a transient state, supplying energy to the system. The system can be an open loop system, however a closed loop control system would be ideal as there would be feedback into the system with use of sensors.

This research paper concluded that, although it is still in its infancy, this concept appears suitable for flow applications in realistic environments. The results showed that of the vertical sided and smooth dimples, the former generate a pair of persistent horseshoe vortices that have common flow towards the surface. It should be noted that such a system would create extra stresses and strains up to 500KPa for a 30% strain; this would need to be taken into account in structural design phases. It concluded that the vertical-sided dimples are more likely to be appropriate for open-loop forcing applications such as flow separation control; however these would be harder to implement as the feedback would need to be analysed. However, due to the nature of vortices, the current actuators are not responsive enough, and therefore a closed-loop control system would give better results. If such a system were to be implemented into an aircraft fuselage, the ideal placement would likely be before an upsweep (Dearing et al, 2007).

However Wind Tunnel testing would require the use of different sizes of EAP's, therefore this would bring about scaling problems for use on a full scale helicopter. There would likely be an added weight and additional power required for the actuators. This would need to be assessed against the drag benefits to understand if such a design would be beneficial.

2.3.3 Anti-Torque Control Systems

2.3.3.1 Fenestron

Shrouded or ducted fan anti-torque designs, which are known as "fenestrons", "fan-in-fin", or "fantail" designs, have been frequently considered over conventional tail rotors, especially for smaller and lighter helicopters, partly for aerodynamic improvement.

The figure below illustrates an industry example for the Fenestron installation device, on EC-155B.

Figure 2.12. Example of a Fenestron installation device on the Eurocopter EC-155B

The Fan-in-fin designs have lower power requirements than an open tail rotor to produce the same amount of thrust. Alternatively, this means the fan-in-fin design can give the same anti-torque and yaw authority with a smaller and perhaps lighter design compared to a conventional tail rotor.

In forward flight the fan-in-fin is shielded from the external flow and the main rotor wake and, consequently, its performance is usually more predictable. The vertical fin surrounding the fan is designed to provide a side force in forward flight and so most of the anti-torque. The aerodynamics of "sense of rotation" and the interference effects of the assembly, which are important for conventional tail rotor, are less important for the fan-in-fin design. However, the possibility of flow separation at the inlet lip of the shroud must be kept in mind, and usually the lip is carefully contoured to avoid such effects (Vuillet & Morelli, 1986).

From a safety perspective, the shrouded nature of the fan-in-fin reduces the possibilities of blade strikes during low-altitude flight operations and also the risk of injury to personnel on the ground.

The larger number of blades on a fan-in-fin design increases the frequency of the rotor noise and this can appear in the helicopter noise spectrum over a range of frequencies to which the human ear is more sensitive. However, at greater distances these higher frequency sounds are more readily absorbed in the atmosphere. Efforts to reduce the noise of fan-in-fin designs through phase modulation using unequal blade spacing have made the fan-in-fin sound subjectively less noisy.

Such a system has the particularity of reducing the frontal area, when compared to a conventional Anti-Torque Control System, and consequently reduce the parasite drag values.

2.3.3.2 NOTAR

There are a number of no tail rotor solutions (NOTAR) that have been developed for helicopters and these can potentially operate in two ways.

The first uses the airflow that is blown onto the tail boom by the main rotors. This is ducted into a system where a variable pitch fan powered by the main gearbox, gives rearward momentum to the airflow, which is exhausted at the end of the tail boom. Using Coanda effect, the airflow passes over the tail boom producing a net force in an anti-torque direction, thus acting as a tail plane. However this system is likely to cause a larger download.

An alternative system is exhaust based and uses main engine exhaust to power an anti-torque capability at the end of the tail boom. Of these two, the exhaust solution would likely be optimal; it uses the engine power more efficiently (20% had been quoted previously for tail rotor power) and there would be no extra download caused by the requirement for an extra air duct. However the problem would likely come from the control system point of view, as the main rotor thrust is not proportional to the tail rotor thrust at all speeds, also there would likely be an added mass due to extra plumbing. This could perhaps be remedied by vectoring the exhaust thrust; this would require a complex and robust design. However, it would likely produce optimal results (Sampatacos et al, 1983).

In figure 2.13 is presented a schematic picture of a NOTAR anti-torque system implemented on the MD500, with description of the direct components involved in the installation.

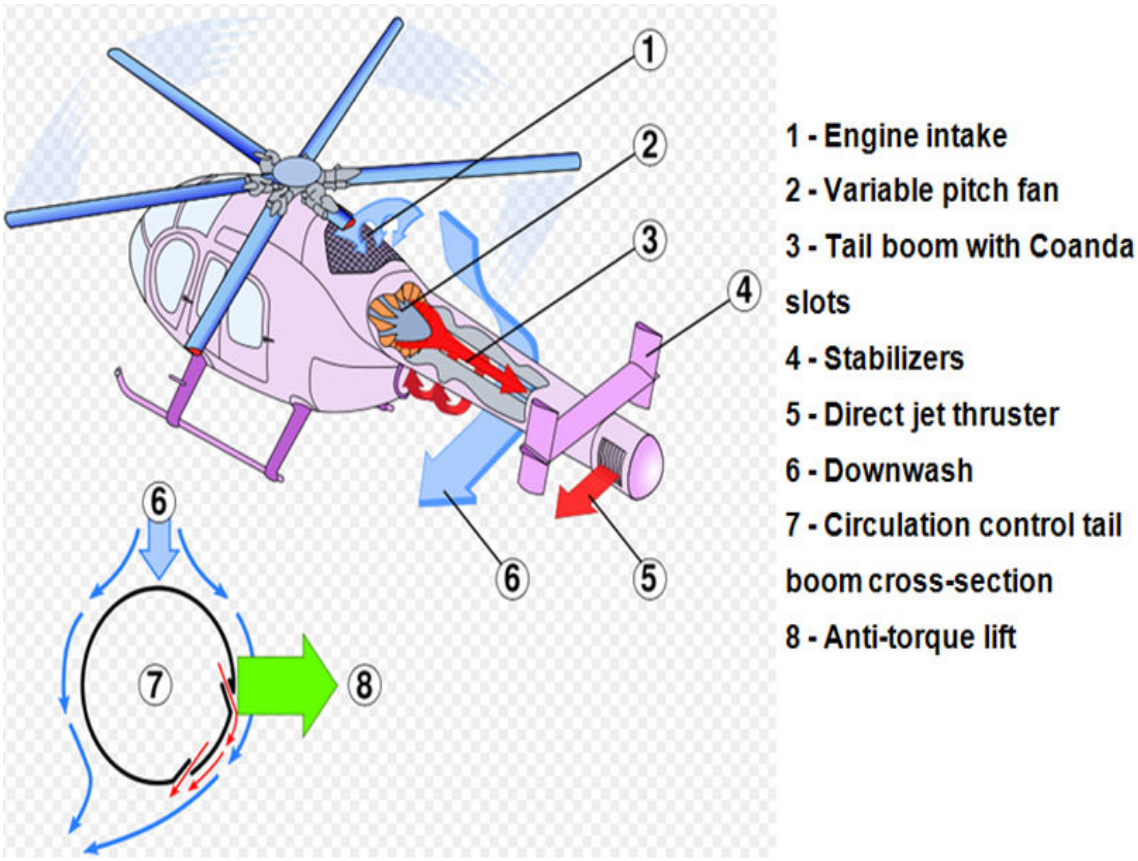

Figure 2.13. Schematic picture of the NOTAR anti-torque system

Of the two methods, the airflow based one is the only one developed and proven with McDonald Douglas MD520/600/900 proving the concept. These aircrafts also benefit from improved safety and improved vibration and noise performance; however they have reduced lifting capabilities.

Should be kept in mind that in this concept, no added drag will be addressed to the aircraft because of the use of an hidden anti-torque control system (relatively to an external flow frontal area).

2.3.3.3 Vectored Thrust Ducted Propeller System

An alternative system that has been developed is a vectored thrust ducted propeller system in the X-49 (Sikorsky Concept). This essentially turns the tail rotor in a rearwards direction, and produces an anti-torque force via the addiction of a rudder.

In the figure below is presented the Sikorsky X-49 concept during a flight test, in forward flight attitude, where is possible to see the two most significant adaptations, the vectored thrust ducted propeller system placing the tail rotor and an additional pair of wings mounted in the fuselage.

Figure 2.14. Sikorsky X-49 concept flight test, based on the S-60

The theory is that the required anti-torque force produced by a tail rotor at higher speeds is reduced; therefore more engine power is directed towards the main rotor. With a ducted propeller system however, the rudder will simply straighten up producing a more forward thrust as well as reduced anti-torque force. The ducted propeller system will lead to less engine power used for lift and more for thrust, so the aircraft would likely fly at a more positive incidence. The reduction in lift led to the need for larger wings on the X-49. At high speeds the helicopter may produce superior results as there

is a direct thrust pushing the aircraft forwards, however at low speed, where tail rotor usage would be at its highest necessity, the ducted propeller system would need to run at a high speed with high rudder angle to produce the required anti torque force, which would be a highly inefficient way of producing this force (Cao et al, 2007). This would lead to the conclusion that this solution would only be viable for long range/high speed transportation, assuming that this solution produces improved cruise results as the system on the X-49 over the S-60 is 700kg.

2.3.4 Considerations for engine Installation Performance Improvements

Taking the various ideas from this entire literature search, there are two forms of engine installation commonly used in turbine engine helicopters. The turbo-shaft engines could be mounted either directly ahead or behind of the main rotor transmission, depending on whether the engines are front or rear drive, but with the addition of angle drive gearboxes the engines could be mounted on both sides. Implementing the engine installation forward or aft avoids increasing the cross sectional area to accommodate the engines but involves technical hitches in either inlets or exhausts. A front mounted engine can use a simple pitot intake, but must exhaust sideways because of back pressure losses, with a significant momentum drag (or jet thrust loss) and disturbance of the flow in the sensitive gearbox/hub area. Rear mounted engines usually involve double bends in their inlet ducts with attendant power losses. These two most common installations are represented in the figure below.

The figure 2.15 illustrate the two most common engine installation implementation, with a forward mounted installation with specific intake filters and side-faced exhausts and an aft mounted installation with a optimized design.

Figure 2.15. Image showing common engine installation mounted ahead, on the EC725 (left), and behind, on the S76 (right), of the main transmission

The engine installations implemented on both sides of the transmission are preferable from weight balance, accessibility and battle damage points of view. The side mounted engine places no restriction on the exhaust or inlet design but this installation tends to increase frontal area and interference drag (particularly on the rotor hub). With engines located on what are in effect stub wings, there is a danger of developing significant vertical forces and attendant induced drag. Any aerodynamic download is objectionable since it must be balanced by an increase in thrust and power of the main rotor system. High fuselage downloads can decrease the aircraft's main rotor flight envelope through the early onset of retreating blade stall flutter. On the other hand, lift produced by the fuselage can unload the rotor and enlarge the aircraft's rotor envelope.

The figure presented below show an heavy-sized helicopter powered by three engines with two different types of installation positioning, two engines centre mounted and one aft mounted.

Figure 2.16. EH-101 showing two different types of engine installation

The helicopter illustrated in figure 2.16 has two different types of engine installation. The outboard engines have obvious potential to generate large lift forces, depending on the inclination of the nacelles to the fuselage. Angles which cause large downloads must be avoided; however, large lift forces will tend to put up super velocities in the hub area, giving an interference drag penalty plus an induced drag on the installation itself.

The engine inlets shown in figure 2.16 are side facing, dictated by the need to avoid ingesting large ice particles shed from upstream elements of the airframe (Mazzucchelli & Wilson, 1991). Pitot type inlets are particularly prone to ice ingestion and require some form of particle separator or plenum while side intakes avoid ice ingestion at the expense of the failure to recover any of the forward flight dynamic head. At helicopter forward speeds there is little penalty in fuel flow due to this latter approach. The main effect is that engine power limits do not benefit from the ram effects of a pitot intake. On a multi-engined helicopter, power limits in forward flight are seldom a problem; however, engine sizes are normally dictated by take off and low speed flight requirements.

Another consideration that has to be taken is the correct exhaust type implemented for each engine installation. In this matter, three important topics needs to be optimized in order to achieve an efficient propulsion system: the direction of the

exhausted air that directly influence lift, empennage impingement jet temperatures and recirculation air to the inlet; exhaust exit area that can influence forward flight parasite drag (at cruise speeds) and hover attitude; exhaust pipe length that have the task to extract the exhausted air to the desired place.

2.4 Industry Examples

2.4.1 Westland Lynx - Helicopter World Speed Record

As a product capability demonstrator by Westland Helicopters Limited, this model had the purpose to show the capabilities of the manufacturer. This topic is based on Design Paper presented by Chief Aerodynamicist Perry (1987).

For this model, was chosen the army Lynx, with its relatively clean skid undercarriage, as the platform for the speed record because of its low basic drag.

The drag reduction made in this project focused into three main categories: removal or fairing of minor excrescences, reduction of momentum drag associated with cooling systems/engine installation, and fairing in the main rotor head area.

Table 2.2. Drag Breakdown at 216kts with a -6º Fuselage Pitch Attitude (Perry, 1987)

ITEM	Lynx AH Mk1	Drag Reduction	Jet Thrust
Body and Tail-Boom	36	/	/
Nacelles	21	/	/
Excrescences	10.7	5	/
Reynolds No Effects	-4	-4	/
Main Rotor Head	65	45	/
Tail Rotor Head	13	/	/
Skids	17	14	/
Aerials	6.5	2	/
Tail Plane	4	10	/
Gurney Flap	/	1	/
Cooling	14.9	5	/
Engine Ram Drag	8.1	8.1	-40
TOTAL D100 (lb)	192.2	166.1	118

The excrescences removed included windscreen wipers, external footsteps, unfaired fittings for weapon and external cargo carriage, unfaired navigation lights and beacons, and all aerials except for one communication antenna. Any of these items could have been redesigned for minimal drag but for purposes of the record flight it was simplest to remove them. Where excrescences could not be removed, careful detailed fairings could often markedly reduce their contribution to aircraft drag. These fairings included front and rear fairings of the undercarriage skids and fairings of the undercarriage strut/fuselage junction, fairings to the rear of the sliding cabin doors, tail plane root fairings and fairings around the non-removable armament attachment lugs.

The cooling drag losses were approached by means of carefully sized inlets, exhausts and general sealing of panel joints particularly in areas of high pressure recovery on the fuselage. Areas of particular interest were tail and intermediate gearbox and cabin cooling where inlets of reduced size were introduced. Keeping in mind that the cabin contained a large tank of water methanol mixture whose vapour was toxic, the cabin air intake was sized to ensure a rearward flow of air within the cabin and exhaust any vapour from an accidental spill or leak safely aft of the crew station. Main gearbox oil cooler inlet scoops were removed and the usual exit into the main rotor head well was modified to direct the exhaust flow aft. Various seals did not restrict their functions.

For the aerodynamic improvement of the engine installation, the prospect of the excess power beyond the transmission capability being wasted lead directly to the consideration of turning the jet pipes aft and reducing their area to provide a direct propulsive force.

The major drag reduction activity involved the fairing of the main rotor head, which although of a hingeless design and therefore relatively clean, still made up a major part of the aircraft's parasite drag. Rotating and non-rotating fairings were used.

The main gearbox forward cowling was reprofiled in order to reduce super velocities in the hub region as well as to shield the control push rods and spider arms which were otherwise difficult to fair. Fairings were developed for the major rotating components with high local drag coefficients. This design work was facilitated by a considerable body of background experience on rotor head drag reduction based on wind tunnel tests on models with rotating heads of various configurations.

The next figure show the Westland World Speed Record G-Lynx in forward flight, where can be seen a group of modifications such as the reduced area of the exhaust outlet, a new tail plane installation, new tension links in the blades, and a much more “cleaned” airframe.

Figure 2.17. Westland World Speed Record G-Lynx in forward flight

2.4.2 Sikorsky S-76

The S-76 helicopter was a program initiated in 1974 with the purpose of design the highest performance level ever reached on a twin-engine light helicopter for commercial use. Therefore, has presented by Fradenburgh (1978), the model main objectives was to (a) meet all the demanded performance objectives, (b) be as aerodynamically cleaned as possible within reasonable cost and weight constraints and (c) be aesthetically pleasant.

The figure 2.18 present the Sikorsky S-75 in hover attitude, and it is possible to notice the carefully shaped streamlined fuselage with retractable landing gear and optimized engine installation.

Figure 2.18. Sikorsky S-75 in hover condition where is possible to notice the various design particularities of this model

Thereby it is possible to identify some good design aspects to reduce parasite drag. In this model, the landing gear is fully retractable, within flush cover doors and no sponsons or local bumps outside the basic fuselage contour are used. All doors and access panels on the aircraft, in fact are flush without protruding hinges or handles, and a substantial effort has been made to prevent leakages. All rivets were used as flush as possible. In the tail, the horizontal stabilizer uses an inverted cambered airfoil for minimum drag at the normal tail download condition, and a vertical fin is also cambered for minimum drag of the fin/tail rotor combination in cruise flight.

Concerning to Cooling Systems, all air inlets were shaped with low-drag lips and the respective exhausts were pointed in the downstream direction. The refrigerating air for the avionics compartment, located in the nose of the aircraft, was drawn from the cabin, dispersed through the avionics components as required and dumped at low velocity into the nose landing gear. Then for cruise conditions, two convergent-nozzles exhausts, one built into each half of the nose wheel cover door panels, provide a negligible system drag by reaccelerating the air to approximately flight speed and exhausting it parallel to the flight direction. With the same principle, the air from the aircraft environmental control unit comes on board through a NACA flush type inlet in the tail cone and exits through another convergent-exhaust nozzle on the bottom of the aircraft.

For the airflow system of the engine installation, the design process was configured separately. The inlets were reduced in size by approximately 25 percent (compared to the engine intake area), reducing the spillage in high speed cruise in order to maintain fully-attached low drag external low. Regarding to the exhaust configuration, new significant features were adopted: where the flow is exhausted straight back along the flight path, and by means of selecting the proper area ratios, is brought back to flight velocity in cruise, reducing the ram drag effect to minimal values. The engine compartment pylon was carefully shaped as well, to accommodate smooth airflow paths from the sides of the aircraft to avoid regions of separation. The cooling air for the engine compartment, which is induced through small auxiliary scoop inlets behind the main inlets, is exhausted in an ejector arrangement surrounding the engine exhaust.

It is interesting to note that the aircraft design follows closely to the specifications set by Boeings research on optimum fuselage shape. This model wasn't influenced by this research but as the S-76 started in production in the mid 70's, it can be considered as a demonstration to improvements obtained by having an optimal shape.

2.4.3 Sikorsky X2

The X2 Technology concept has been developed by Sikorsky, addressing a new coaxial rotor model with pusher blades, with and a single seat proof concept variant already successfully tested in earlier 2008. The idea is to provide a helicopter with a higher range and speed in cruise without compromising the low speed characteristics, in effect to provide tilt rotor high speed performance with conventional helicopter low speed performance.

The helicopter higher speed and efficiency is due to a new type of rotor that does not have the problem of sonic blade tip, this is achieved by a fly-by-wire active blade incidence control technique that slows the blade down at higher speeds. Although most of innovation comes from the rotor blades, as the cruise speed will increase, parasite drag will become greater leading to a greater importance of the fuselage drag, meaning that the final designs will be quite aerodynamic, even for the heavy lift variants.

This figure below represents a table of multirole combinations for the new Sikorsky X2 Technology Demonstrator and the expected specifications for each one.

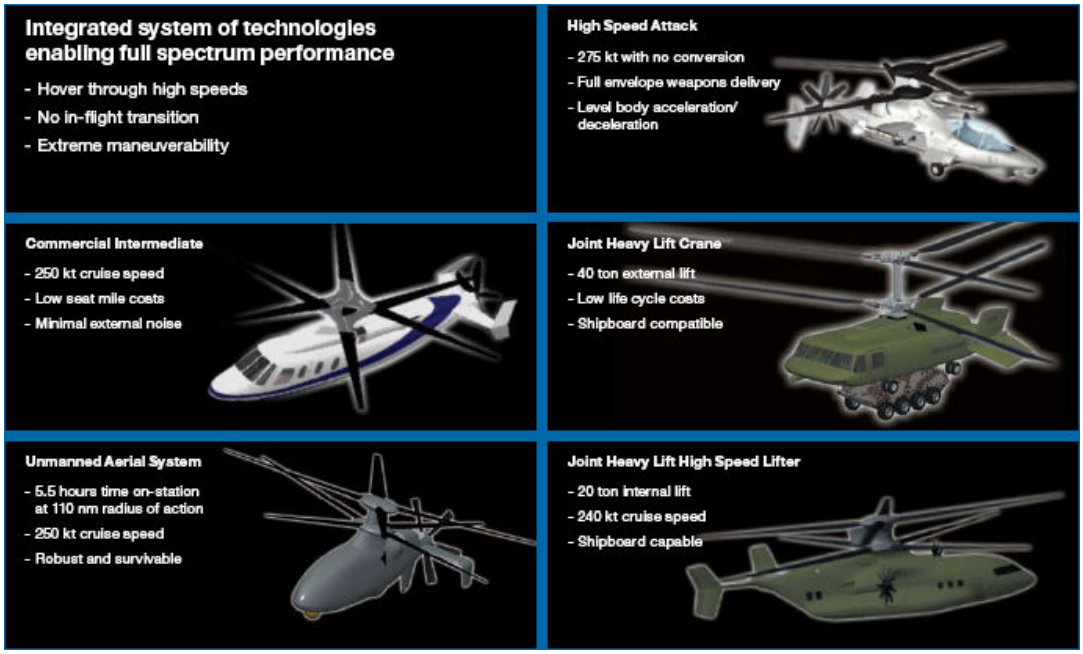

Figure 2.19. The multirole combinations for the Sikorsky X2 Technology Demonstrator

In this way, this concept will gather innovation of a new coaxial hub completely faired and a refined streamline airframe. As a result, Sikorsky plan is to design, develop and launch a coaxial-rotor helicopter capable of cruising at 250kt, over a 700nm (1,300km) range.

2.4.4 Aerospatiale SA 365N Dauphin

From Bristol University, Roesch presented an overview through the improvements made on the aerodynamic design of the SA 365N during its development.

The SA 365N is a high performance twin engine helicopter of the new generation, specifically designed for corporate and off shore operations. A high gross weight to empty weight ratio and a large internal fuel capacity make large payloads over long ranges possible. A careful design of the fuselage shape and of the engine inlets has

produced a fast, clean aircraft with an unusually low level of parasite drag and very low fuel consumption, resulting in high transport efficiency (Roesch & Vuillet, 1981).

The next figure show the Eurocopter AS-365N (SA 365N), presenting the overall optimized modifications made relatively to the old variant of the “Daphin”.

Figure 2.20. Eurocopter AS-365N (SA 365N)

During the development of the SA 365N, important aerodynamic refinements of the airframe were made in order to reduce parasite drag. The general streamlining of the fuselage was improved by reducing the boat tail angle at the intersection of the fuselage with the tail boom and by reshaping the blunt nose of the SA 365C into the more popular “corporate” nose shape which offers room enough to house a radar antenna and various IFR communication and navigation equipment.

A retractable tricycle landing gear on the SA 365N replaces the fixed landing gear of the SA 365C. Retractable footsteps for cabin access were also installed.

The emergency floatation gear on the SA 365N was integrated into the fuselage so that it does not create any additional drag when folded.

A special pylon fairing was developed during flight testing to reduce rotor head-fuselage interaction drag and attenuate the hub wake by reactivating the flow behind the hub. The SA 365N pylon fairing design has evolved from hours of testing in the wind

tunnel. It incorporates several features designed to depress the wake downwards and to attenuate the turbulence by introducing fresh, relatively steady air, into the core of the wake. Drag measurements for this configuration showed good correlation with the total pressure measurements. The hub cap alone has little effect on parasite drag. With the pylon fairing on, the drag area was reduced by 0.15 m^2. (Roesch, 1980)

The engine fairings on the SA 365N were completely redesigned to accommodate new dynamic air intakes minimizing engine installation losses in replacement of the SA 365C static inlets. The objective was to develop aerodynamically efficient inlets characterized by a high dynamic pressure recovery in forward flight and a very low level of distortion and turbulence in all flight configurations.

The air cooler inlet of the main gearbox and engine oil, located between the engine intakes, has also been redesigned. The inlet has been moved forward and is reduced in size to minimise drag. The new duct design incorporates a larger diffuser. The cooling air is exhausted through a converging nozzle at the rear of the pylon fairing. Comparative drag measurements have shown that significant parasite drag reductions were obtained with the dynamic air intake arrangement.

Table 2.3. Airframe Parasite Drag Reduction on SA 365N (Roesch, 1980)

Component	SA 365C (m2)	SA 365N (m2)	Nature of Drag Reduction
Horizontal Stabilizer	0.024	0.024	
Tail Fin, Side Fins & Fenestron	0.142	0.142	
Footsteps	0.03	0	• Retractable
Landing Gear	0.09	0	
Rotating Main Rotor Head	0.66	0.51	• Pylon Fairing
Fuselage & Engine Cowlings	0.454	0.374	• Improved Streamlining • Reduction of Boat Tail Angle at Fuselage/Tail-Boom Interaction • Oil Cooler Inlet Modification • Dynamic Engine Inlet Arrangement

The overall improvements to fuselage aerodynamics alone led to a parasite drag reduction of about 14.2%.

2.4.5 Mil Mi-38

The Mi-38 prototype took off for the first time on 22 December 2003, and the first test flight took place on 25 August 2004. The helicopter is intended for the transport of 30 passengers (maximally 44). In the cargo capacities in the cabin, it can take seven tonnes versus the four the Mi-8MTV has. The Mi-38 is larger than its predecessor: its maximum takeoff weight is 15.6 tonnes (the Mi-8MTV is 11 - 13 tonnes.) At the same time, however, owing to the perfection of the aerodynamics, drag has been decreased by two times. The new helicopter develops a speed of 275 - 285 km/h (the Mi-8MTV is 210 - 230 km/h). The specific servicing effort also has been decreased more than two times, the noise level by four , vibration parameters by six times, and service lives of basic systems increased by four to six times.

In the figure 2.21 is shown a Mi Mil-38 climbing with a high pitch attitude during a product exhibition flight, where it is possible to observe the improvements made on the streamlined fuselage and new designed engine installation.

Figure 2.21. Mil Mi-38 during a product exhibition flight*

As the last validated to production helicopter by Mil, the Mi-38 was designed as a direct replacement of the Mi-8/Mi-17. This concept focused much of its attention to aerodynamics, from which can be highlighted three main areas: an overall care with

doors and rivets designed as flush as possible, the clam shell rear ramp doors & short ramp provide a much more streamlined design, and a completely new pylon/engine installation area for rotor/fuselage interaction improvements. Due to the aerodynamic improvements, was evaluated that the Mi-38 has half of the total parasite drag over its predecessor.

2.4.6 Kamov Ka-92

The pusher propellers helicopter concept will be the level-flight propulsion configuration of choice for Russian manufacturer Kamov for a new breed of high-speed rotorcraft to fly in the 2015 timeframe. In 2008 Russian rotorcraft specialists revealed high-speed helicopter concepts competing for government allocation for development of new rotorcraft technologies. Kamov has two concepts: the Ka-90 and Ka-92.

Concerning to the Ka-92 concept, a range of 1,200-1,400km is required, for cases like when a helipad at destination temporarily closes down, perhaps because of weather conditions, forcing the crew to return to base without refuelling. Another distinct market exists in remote territories with undeveloped aerodromes. Such areas are served by helicopters that maintain regular passenger and cargo services with flights lasting up to 3h. This model would be able to shorten flight time substantially, making a return flight possible with no special infrastructure in place at the destination.

Designed to accommodated up to 30 passengers, the Ka-92 will have a range of 1,400km at 227-243kt cruising speed. The maximum take-off weight will be about 15,000kg, and the engines will drive the coaxial main rotor and counter-rotating coaxial pusher propellers in the rear fuselage which will give the Ka-92 a speed boost in level flight and provide torque balancing.

Shown in the figure below is a mock-up of the Kamov Ka-92 concept presenting the guidelines followed to achieve the efficient design planned.

Figure 2.22. Kamov Ka-92 mock-up concept to demonstrate the project guidelines

According to the designer, it will be essentially a new machine with much higher aerodynamic qualities and the small specific charge of fuel. Therefore, to achieve these objectives, this model will have a carefully streamlined airframe with an improved utility cargo door in the after-body and a retractable landing gear. Simultaneously, the Ka-92 will have a fully faired coaxial rotor hub to improve the aerodynamic characteristics.

Chapter 3

ANALYTICAL RESEARCH

3.1 Active Tailplane

3.1.1 Introduction

The first half of the Analytical Research is focused on heavy-sized helicopter Tailplane. Given that the Clean Sky project looks into the drag improvements on helicopters airframe, this research gives one theoretical approach to set an Active Tailplane on the aircraft that can trim the fuselage incidence to an optimal position during the whole flight envelope and consequently minimize the effective drag penalty by the tailplane on the helicopter.

This concept already made his first step on production helicopters. A common example can be seen on the Apache YAH-64 tailplane (stabilizer), where was implemented a system to set two independent positions in terms of incidence. This device is characterized by a horizontal stabilizer that changes the incidence according to the flight attitude. Consequently, it has a system integrated that measures the forward velocity through three separate devices and then setting the stabilizer to -10 degrees during forward flight or to 35 degrees during hover and vertical flight conditions. With this improved device, the tailplane produces less downwash during hover in the first setting angle and his trimmed for forward flight in the second setting angle (Prouty & Amer, 1982).

During forward flight, helicopters normally fly with the fuselage at a variable pitch attitude relatively to the free stream direction, depending on the on the flight velocity and the CG position.

On the graph below is presented a simulation that shows the variation of the fuselage pitch attitude depending on the aircraft velocity for three different CG positions.

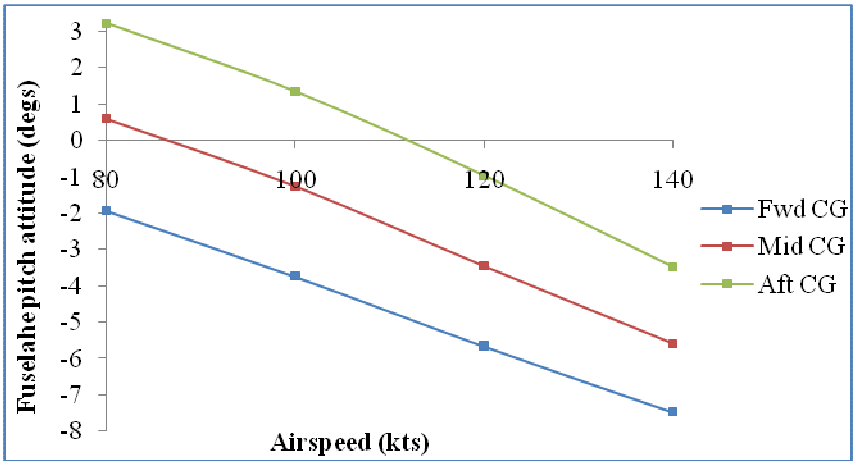

Figure 3.1. Variation of the fuselage pitch attitude depending on airspeed for three CG positions

3.1.2 Simulation

The simulations done during this subject of the Analytical Research has been taken in order to evaluate the aerodynamic characteristics of a theoretical Active Tailplane that could trim the fuselage pitch attitude of a heavy-sized helicopter during forward flight and compare the power/fuel consumption data (presented on appendix).

This analytical work was developed from the FDS program using different inputs for the airspeed, longitudinal CG position, tailplane setting angle (fixed for three degrees on the production model) and for the flight altitude, as it can be seen on the next table.

Table 3.1. Variable input values used to evaluate the Active Tailplane simulation

CG=-0.155m				CG=0.075			CG=-0.385
SL				4000ft			
80kts	100kts	120kts	140kts	80kts	100kts	120kts	140kts
5	5	5	5	5	5	5	5
3	3	3	3	3	3	3	3
0	0	0	0	0	0	0	0
-5	-5	-5	-5	-5	-5	-5	-5
-10	-10	-10	-10	-10	-10	-10	-10
-15	-15	-15	-15	-15	-15	-15	-15

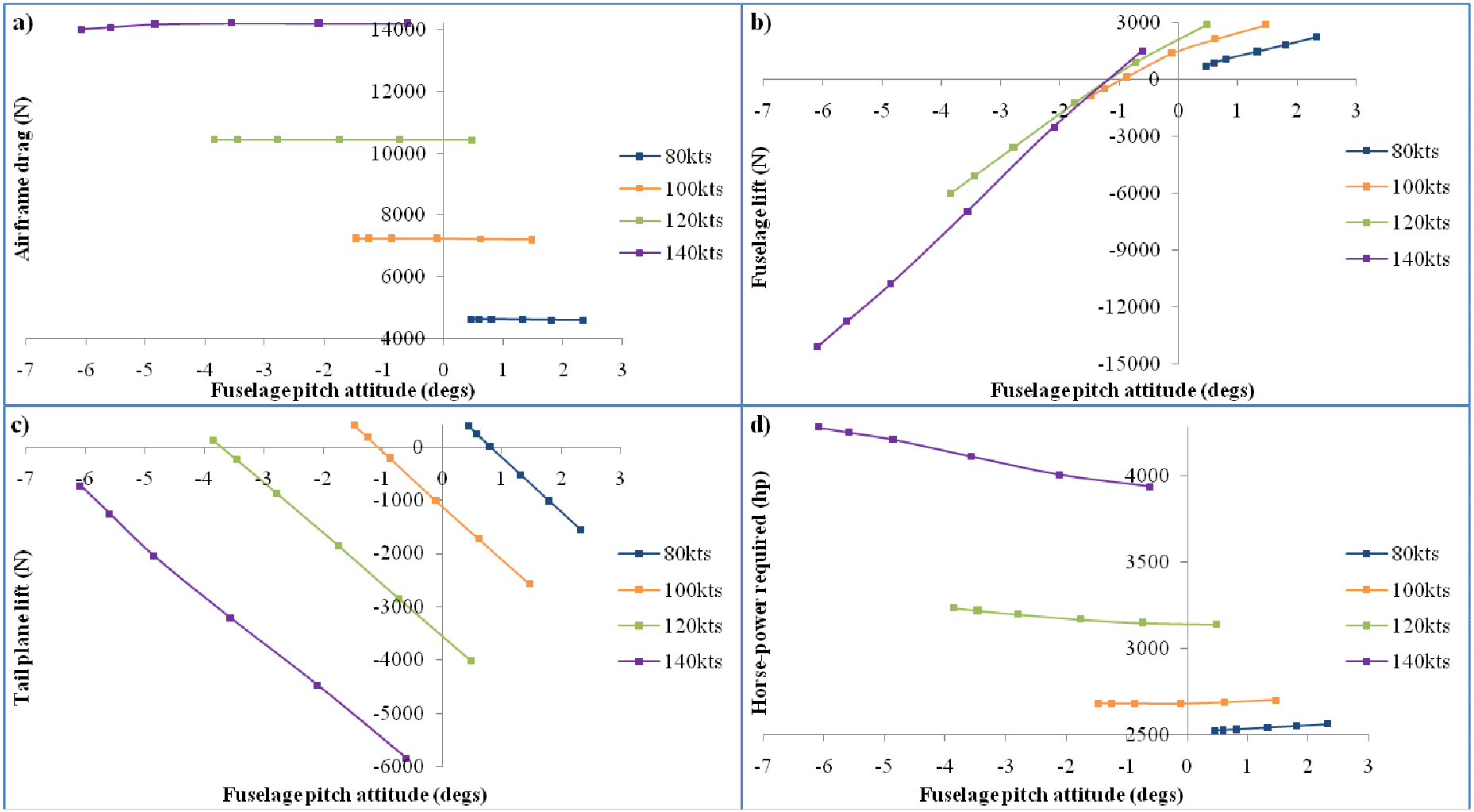

Figure 3.2. Graph representation of the fuselage pitch attitude, depending on: a) airframe drag, b) fuselage lift, c) tailplane lift and d) horse-power required; flying at SL with middle CG position.

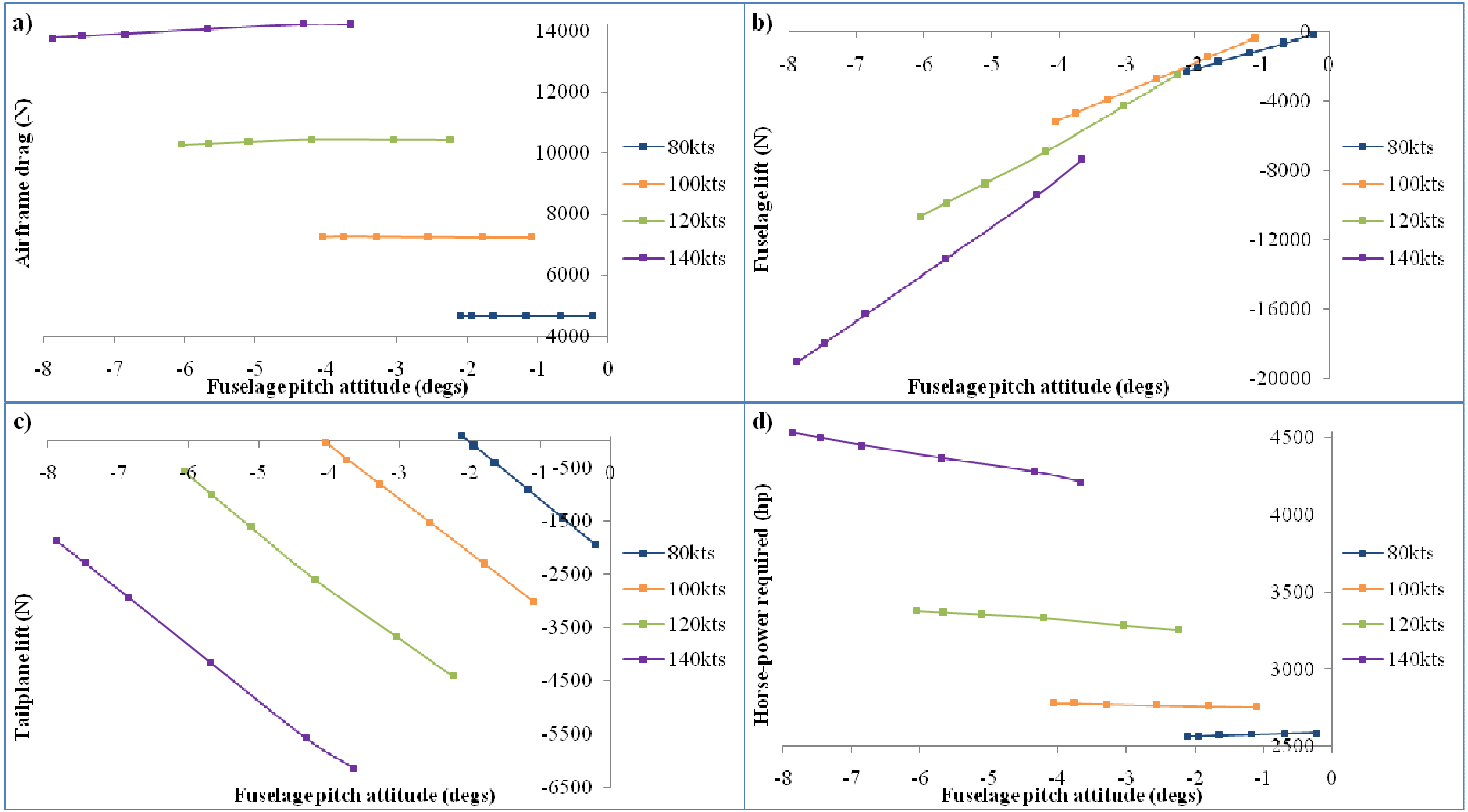

Figure 3.3. Graph representation of the fuselage pitch attitude, depending on: a) airframe drag, b) fuselage lift, c) tailplane lift and d) horse-power required; flying at SL with forward CG position.

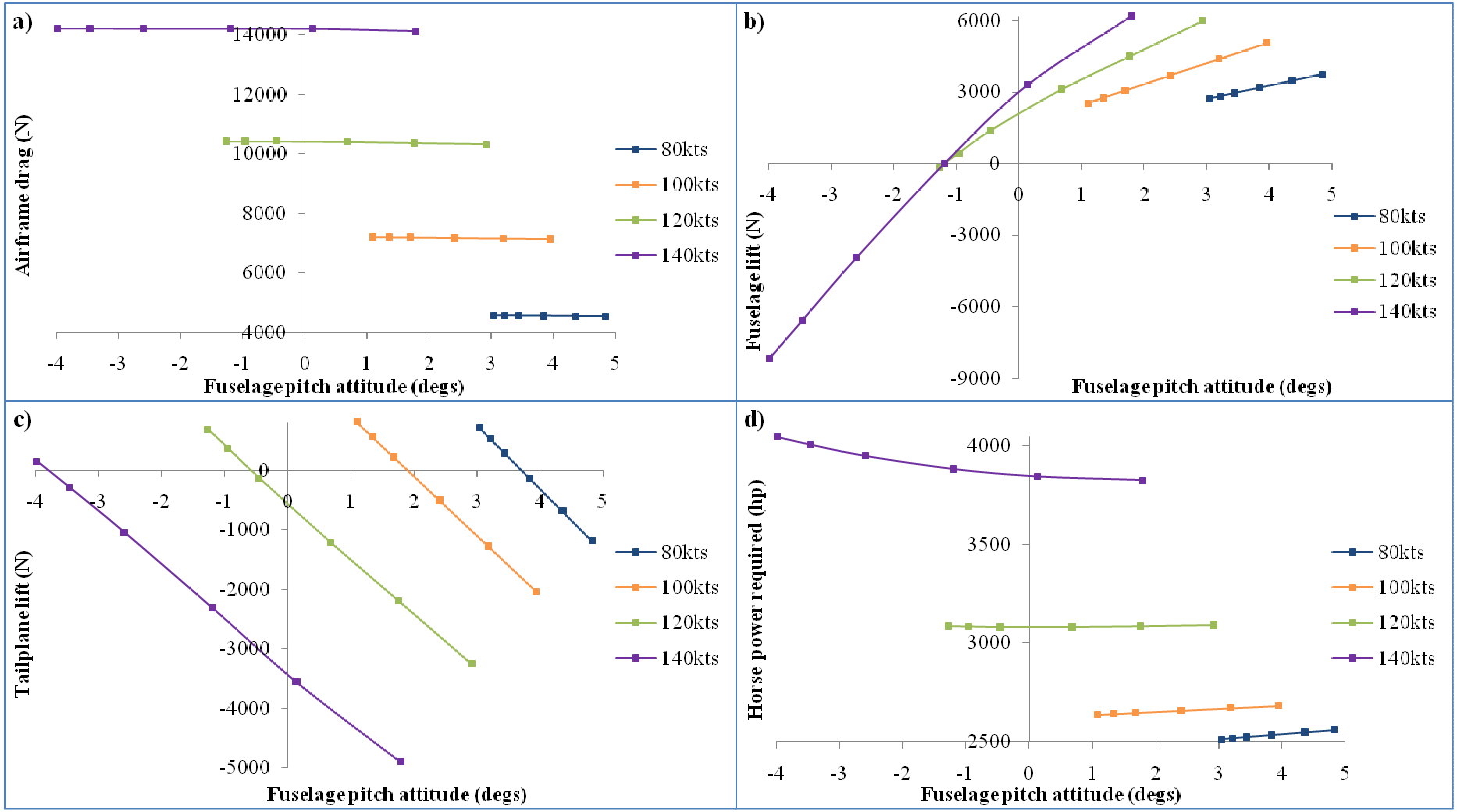

Figure 3.4. Graph representation of the fuselage pitch attitude, depending on: a) airframe drag, b) fuselage lift, c) tailplane lift and d) horse-power required; flying at SL with after CG position.

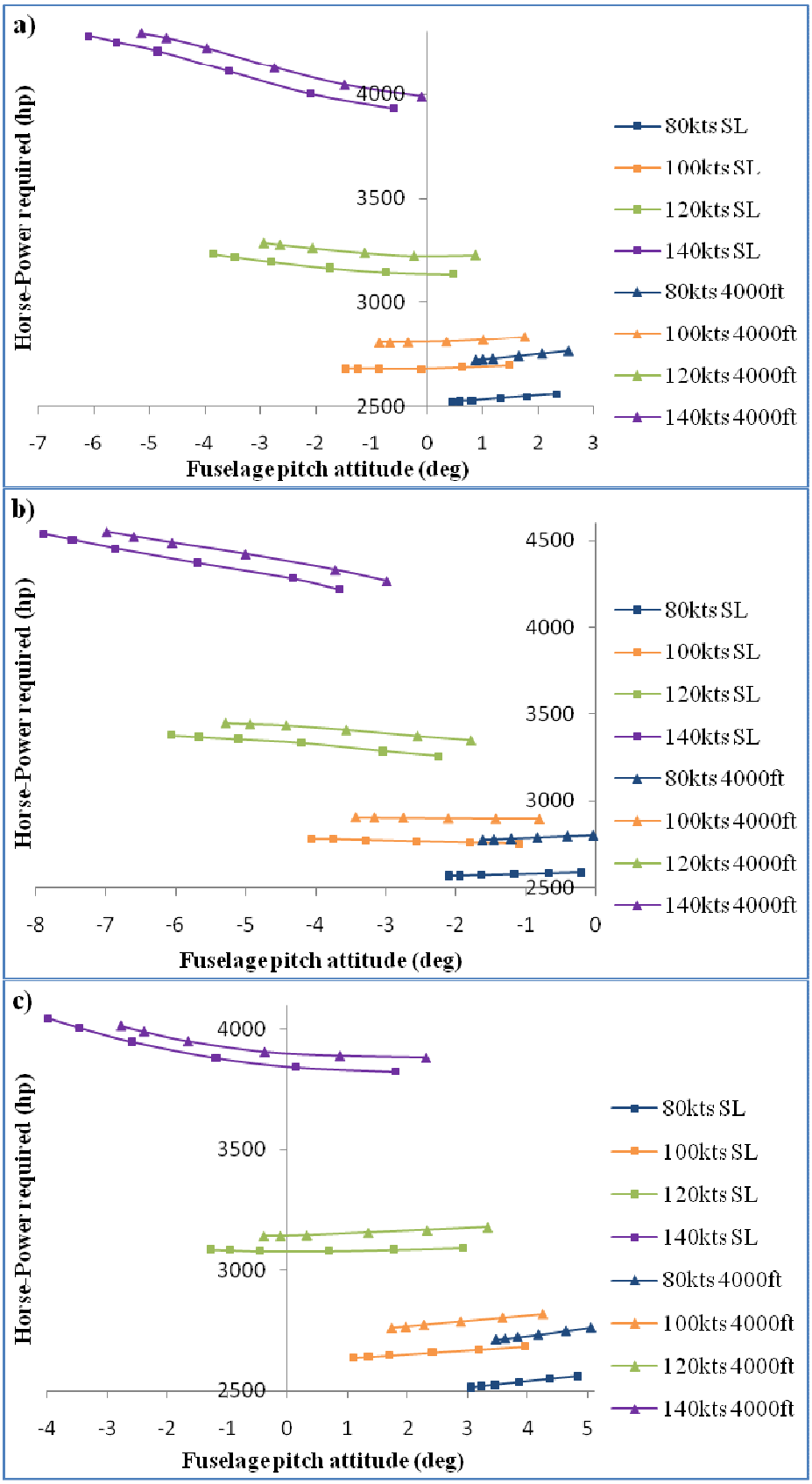

Figure 3.5. Graph representation of the fuselage pitch attitude, depending on horse-power required, for: a) middle CG position, b) forward CG position and c) after CG position; comparing the data obtained between SL and 4000ft.

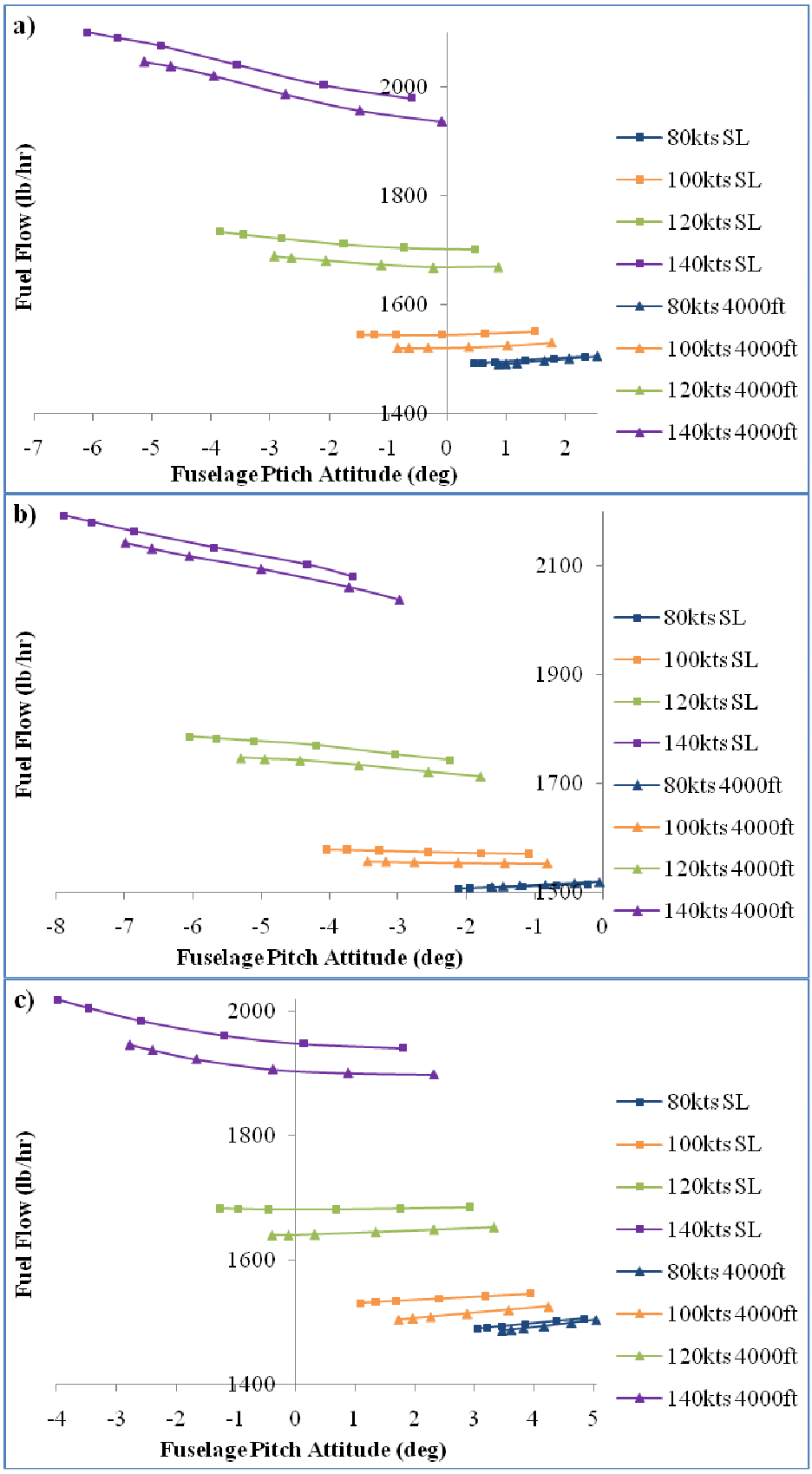

Figure 3.6. Graph representation of the fuselage pitch attitude, depending on fuel flow, for: a) middle CG position, b) forward CG position and c) after CG position; comparing the data obtained between SL and 4000ft.

3.1.3 Savings

Table 3.2. Presentation of the optimum tailplane angle for each flight configuration analysed, with the respective fuel flow and horse-power required and saved

Configuration	Tailplane Angle(deg)	Velocity(kts)	Horse-Power Saved(%)	Horse-Power Required(hp)	Fuel Flow Saved(%)	Fuel Flow[7](lb/hr)
SL CG = -0.155m	5	80	0.087	2523.3	0.048	1492.68
	-5	100	0.067	2681.8	0.037	1545
	-15	120	2.507	3138.7	1.62	1701.54
	-15	140	8	3933.7	5.56	1979.79
SL CG = 0.075m	5	80	0.074	2566.7	0.042	1507.02
	-15	100	0.864	2754.3	0.52	1569.45
	-15	120	3.438	3257.5	2.25	1743.12
	-15	140	6.775	4218.6	4.81	2079.51
SL CG = -0.385m	5	80	0.187	2515	0.105	1489.95
	5	100	0.155	2638	0.088	1530.54
	0	120	0.104	3080.9	0.066	1681.32
	-15	140	4.757	3823.7	3.28	1941.3
4000ft, CG = -0.155m	5	80	0.095	2725.1	0.062	1491.03
	5	100	0.021	2807	0.014	1520.52
	-10	120	1.588	3224.9	1.07	1668.72
	-15	140	7.037	3988.7	5.22	1936.92
4000ft, CG = 0.075m	5	80	0.097	2775.6	0.066	1509.21
	-15	100	0.332	2895.3	0.22	1552.32
	-15	120	2.767	3349.8	1.89	1712.43
	-15	140	6.076	4266.2	4.62	2036.82
4000ft, CG = -0.385m	5	80	0.17	2711.9	0.11	1486.29
	5	100	0.203	2762.6	0.13	1504.53
	5	120	0	3144.1	0	1640.43
	-15	140	2.847	3881.3	2.09	1898.46

[7] The Fuel Flow obtained for the data presented on this Thesis was taken from the table of fuel flow per engine, presented on appendix.

The results presented on the table above were gathered from the FDS data considered for this analytical research. It shows the optimal tailplane angle, compared to the production fixed 3º tailplane angle, which can reduce the horse-power required and the fuel flow for all the flight configurations analysed.

3.1.4 Analysis

Considering a new concept to fit on a tailplane of a heavy-sized helicopter, the results obtained by this simulation indicate that theoretically it is possible to improve the performance properties of the aircraft after implementing this system.

For the range of tailplane angles used on the simulation, there are a reduction on the horse-power required and consequent fuel flow on 95.83% of the flight configurations analysed.

As it was presented on first chapter, the objective of this project is to reduce the drag/fuel consumption of a heavy-sized helicopter during forward flight and his consequent environmental impact. The data obtained shows that the most promising savings concerns to all the optimized 140kts forward flight configurations. Looking for the results obtained by the range of forward velocities used, is possible to understand that savings can be reached by increasing the tailplane angle for the lower forward velocities, 5degrees at 80knots, and decreasing the tailplane angle for the higher forward velocities, -15degrees at 140knots.

3.2 Cooling Systems

3.2.1 Introduction

On any large powered mechanical device, there is always a strong consideration for the required cooling. Helicopters are no exception, and they require multiple cooling systems; for this research, these include gearboxes cooling, air conditioning systems and avionics refrigeration. The cooling systems are generally kept independent from one

another, due to differing location of the systems; therefore this means that there is likely to have a considerable number of inlets and exhausts over the whole aircraft.

Typical cooling inlets generally differ in size and type. There are two distinct types of inlets: suction and ram type inlets. Suction based inlets are discreet to the profile of the aircraft and would likely consist of grille located parallel to the surface with a variable flow rate fan inside of the duct producing suction. These inlets are optimal for lower required flow rates; however they are less optimal for higher flow rates as a larger suction force and grille area will be vital to produce the required flow rate, these two enlargements requiring more power and space.

The figure below shows the suction type flush ambient air intake for the cabin cooling system, on the port side of the fuselage.

Figure 3.7. Picture of the port side of the fuselage showing the flush ambient air intake

Ram type inlets use a shroud and are indiscreet, and even without taking into account the momentum drag, they would produce their own drag themselves. These types of inlets are suited for devices that need a high momentum flow; and additionally they also have the benefit of not requiring power. The ram type inlets are less optimal for low flow rates, unless the geometry of the inlet can be varied in a retractable nature, and the flow rate cannot be as easily controlled by a static system.

The next image shown illustrates the ram type inlet used on the avionics cabinet cooling system, which includes two independent intakes underneath.

Figure 3.8. Picture of the avionics cabinet cooling system intake used

The other concern about the cooling systems is the momentum drag, but this problem can be offset by a certain amount if the exhaust systems were to be placed in a rearwards facing position, where net momentum drag effect can be reduced. However the implications of this can cause problems, redirecting the flow in a free-stream direction from a perpendicular direction would produce a profile drag on the exhaust itself, possibly negating the added benefit. A solution could be to extend the flow of the exhaust to a point rear of the aircraft likely to be close to the upsweep and exhaust flow there; though this could add additional weight and complexity due to the required extra plumbing on the aircraft.

As is the case with many exhaust based systems, a grille maybe used; however the method of exhausting the air away from the free-stream can cause an added drag to the aircraft by inducing the effect of flow separation. This can be explained by the fact that the airflow out of the system has a net free-stream direction velocity of zero, this airflow out; upon contact with the free-stream airflow is immediately accelerated. This causes a low momentum flow over the rear of the aircraft and it causes a higher drag due to induced flow separation. Internal losses will not account for such a drag loss. It should also be noted that in some cases placing the exhaust in a rearwards direction can produce undesirable aerodynamic properties over the remaining fuselage and tail boom, this may lead to instability or even added drag itself; still this is design dependent and may not be the case, depending on flow speed.

This section looks into the changes in cooling systems that can be done through design improvements on the intakes, exhausts and duct net complexity.

3.2.2 Results and Savings

Table 3.3. Properties of the Cooling Systems considered for this research

System		Inlet Flow [kg/s]		Inlet Drag [N]		Outlet Flow [kg/s]		Outlet Area [m^2]	Outlet Drag [N]		Outlet Velocity[m/s]	
		-14°C (OAT)	15°C (OAT)	-14°C (OAT)	15°C (OAT)	-14°C (OAT)	15°C (OAT)		-14°C (OAT)	15°C (OAT)	-14°C (OAT)	15°C (OAT)
MGB		1.225		88.164		1.225		0.0145	3.748		68.96	
IPCS		0		0		0.123725		0.00951	7.597		10.62	
ACCS[8]		0.275625		19.884		0.123725		0.00766	0		13.18	
						0.1519		0.00766	0		16.19	
ACSP[3]		0.378		27.071		0.378		0.03002	0		10.28	
Pack	APU Bleed Air	0.227	0.718	16.392	51.644	0.227	0.718	0.01236	12.946	17.663	14.99	47.42
	Engine Installation Bleed Air	0.173	0.68	12.411	48.926	0.173	0.68		10.482	18.435	11.43	44.91

Table 3.4. Theoretical improvements that can be made on Cooling Systems, globally and for each group

	Systems	Flow [kg/s]	Velocity [m/s]	Inlet Drag [N]	Exhaust Drag [N]	Total Drag [N]	Savings [%]
Global	New	3.4	72.02	244.608	0	244.608	15.749
	Fitted	3.4	72.02	235.689	47.443	283.132	
Group ECS	New	2.175	72.02	156.548	0	156.548	22.147
	Fitted	2.175	72.02	147.525	43.694	191.219	
Group MGB	New	2.175	72.02	88.164	0	88.164	4.251
	Fitted	2.175	72.02	88.164	3.748	91.912	

[8] For the purpose of this research, the outlet drag of ACCS and ACSP was considered as zero because of the respective outlets that exhaust the air perpendicular to the free-stream direction.

All the data presented above was taken from AW reports with proper product specification. It was converted in SI units and manipulated in order to gather the information needed for this research.

The results obtained were divided in three different sections: Global, Group ECS and Group MGB; to give a better understanding of the aerodynamic changes that need to occur to improve Cooling Systems. The theoretical results of the new cooling systems approached on this thesis were considered for forward flight condition at a velocity of 140knots. These new systems reduce the parasite drag and at the same time almost neutralize the interference drag produce by the outlets that exhaust the air perpendicular to the free-stream direction.

3.2.3 Analysis

In order to achieve promising improvements on the reduction of heavy-sized helicopters parasite drag, one of the areas considered was the cooling systems.

This section of the Analytical Research looks into an improved concept that can reduce the parasite drag and reduce the flow disturbances around the airframe. The results presented on table 3.4 shows two different methods considered that can achieve those objectives.

The first method is a Global Cooling System that gathers all the existing systems fitted on the production model, using just one optimised inlet and outlet. The outlet is considered to exhaust the air backwards, at the same velocity as the cruise speed, then producing zero drag.

The second method is an improved Cooling System divided in two main systems: ECS and MGB. This method is similar to the first one, but separates the MGB from all the ECS systems.

The results show the benefit taken from those two methods in terms of drag, considering at the same time that this method reduce the turbulence around the airframe.

Chapter 4

CONCLUSIONS

Looking to achieve state-of-the-art for helicopters on the XXI century, a direct conclusion is that the most aerodynamically efficient designs are generally long range corporate passenger carrying helicopters, and this is due to the need for reduced travel time and cost.

As presented by the literature search developed in this thesis, the fuselage parasite drag accounts for 60-70% of the total parasite drag of the aircraft, In order to achieve an optimised design, the guidance to reduce the fuselage parasite drag should address the following:

- The nose section of a helicopter should be kept with a corner radius to fuselage width ratios below 0.1 to avoid a noticeable increase in parasite drag.
- Rectangular Cabin sections on helicopters produce four times more fuselage parasite drag than circular airframe sections.
- Utility helicopters after-body represent the largest drag contribution area of the airframe. The flow separation at the upsweep section of the fuselage is avoided for contraction ratios (l/d) above 2.0, consequently reducing the inherent pressure drag.
- A retractable landing gear delete the parasite drag of this component, but if an external landing gear is required, a skid gear can reduce the drag by 40% when compared to fixed wheeled gear.
- The antennas with airfoil section can originate values of parasite drag 4% lower than antennas with cylindrical section.
- Wind tunnel test developed on the CH-46 found 8% of drag reduction of the basic fuselage, giving also directional stability to the aircraft, when strakes were applied at cambered rear loading after-body.
- The use of deflectors avoids the change between vortex and eddy flow at the fuselage upsweep at negative fuselage incidences, reducing the drag penalty in this section.

- Implementation of Synthetic Jet Actuators at the fuselage rear ramp can reduce the fuselage parasite and interference drag by 10% with 40% reduction in cruise download.

To meet the goals demanded for this guideline, there are some possible side effects, which include:

- A method that reduces drag (such as reducing flow separation at a rear upsweep) may result in a reduced lift and altered pitching moments.
- The changes in lift and drag at certain areas will probably affect the flight dynamics of the aircraft, depending on the severity of the change, a restoring moment would likely have to be produced by either the pilot controls or an alternative device. This change in dynamics could cancel out the benefits of the increased aerodynamic performance of a component.
- Any drag reduction method would probably result in an increase in weight, and in the case of active methodologies, power. In both cases, more fuel burn would be required, especially at low speeds, to overcome this detriment.
- The added weight due to the drag reduction device/s will also affect the trim of the aircraft, which must be taken into account at design stage.
- If exhaust flows are facing rearwards, there is the possibility of interference with the flow over the tail of the aircraft, which can cause structural problems.

Industry examples of helicopters with some of the drag reduction methodologies presented in this thesis, shown total drag reductions of 38.6% for the G-Lynx and 24.5% for the SA 365N.

For heavy-sized helicopters, an active horizontal stabilizer can produce some significant improvements over the static horizontal stabilizer. However this is only the case when the trimmed flight angles are far away from zero, as it can be noted for a forward CG cruise flight condition. It should also be noted that, at higher speeds, the reduction in power is much greater; consequently this method can reduce the fuel flow required by 2.1-5.6% during cruise flight at 140kts. The gradient of power per degree increases with speed, and this could mean that on high speed helicopters, for improved range performance, an active tailplane could be implemented to significantly improve the performance.

On ECS and MGB Cooling Systems, current practice is for the flow to be exhausted rearwards at approximately free-stream velocities, this reduces the net ram drag close to zero at cruise. A system that gathers all of the existing Cooling Systems in a new unified system could theoretically reduce its drag by 15.75%. The S-76 design case, which exhausts the MGB cooling flow at approximately free-stream velocities, demonstrates that it is realistically possible to exhaust flow at free-stream, and there is probably an overall performance benefit for doing this. It is better to implement such a system in the design stage, where cooling systems can be designed to operate with high fluid velocities.

Recommendations

Concerning to future work on the GRC2 project, there are some possible steps that could address the following:

- Evaluate design solutions with special attention on the implementation of the guidelines presented on this thesis, making the step to achieve an optimised shape that can considerably reduce the amount of parasite drag normally found on heavy-sized helicopters. Continue the research and analysis presented in this thesis through all active and passive methods to reduce the parasite drag with the purpose of implementing it on this project.

- Continue the research around the active horizontal stabilizer with more refined ranges of velocities and horizontal stabilizer lift values used for each flight condition. Analyse the type of tailplane configuration needed for this concept and make proper trade-off studies with the aim to evaluate a more accurate benefit of this system.

- Continue the research and analysis for Cooling Systems to appraise the specifications demanded for an improved concept, presented in this thesis, which will consist in a global system to reduce as much as possible the airframe parasite drag. Understand and evaluate the feasibility of designing this new system in order to find the final benefits taken from such improvements.

- Conduct research and analysis work into engine installation design for maximizing engine installed performance and minimizing installed drag.

References

- Ballin, M.G., 1987. “Validation of a Real-Time Engineering Simulation of the UH-60 Helicopter”, NASA TM-88360.

- Ben-Hamou, E., Arad, E., Seifert, A. 2007. “Generic Transport of Aft-body Drag Reduction using Active Flow Control”, Flow Turbulence Combust, No. 38:365-382.

- Cao, Y., Li, D., Zhang, Q., Bian, H. 2007. “Recent Development of Rotorcraft Configuration”, Beijing University of Aeronautics and Astronautics, Beijing 100083, P.R. China.

- Clark, R.D., Wilson, F. 1980. “A Study of the Effect of Aft Fuselage Shape on Helicopter Drag”, Proceedings of the 6th European Rotorcraft and Powered Lift Aircraft Forum, Paper No. 50, Bristol, England, September 16-19.

- Dearing, S., Lambert, S., Morrison, J. 2007. “Flow Control with Active Dimples”, The Aeronautical Journal, Paper No. 3174, pp. 705-714.

- Duhon, J.M. 1975. “Cost Benefit Evaluation of Helicopter Parasite Drag Reduction”, Proceedings of the 31st Annual Forum of the American Helicopter Society. Special Report Presented by the AD HOC Committee on Rotorcraft Drag. Washington, D.C., May 14-15.

- Epstein, R.J., Carbonaro, M.C., Caudron, F. 1994. “Experimental Investigation of the Flowfield about an Upswept Afterbody”, Journal of Aircraft, Vol.31, No. 6:1281-1290.

- Fradenburgh, E.A. 1978. “Aerodynamic Design of the Sikorsky S-76 Helicopter”, Proceedings of the 34th Annual Forum of the American Helicopter Society. Washington, D.C., May 15-17.

- Gatard, J., Costes, M., Kroll, M., Renzoni, P., Kokkalis, A., Rocchetto, A., Serr, C., Larrey, E., Fillipone, A., Wehr, D. 1997. "High Reynolds Number Helicopter Fuselage Test in the ONERA F1 Pressurized Wind Tunnel", Proceedings of the 23rd European Rotorcraft Forum, Dresden, Germany, September 16-18.

- Gaudet, L. 1987. "An Assessment of the Drag Reduction Properties of the Riblets and the Penalties of Off-Design Conditions", Royal Aircraft Establishment, Technical Memorandum Aero 2113, August.

- Gleize, V., Costes, M., Geyr, H.F., Kroll, N., Renzoni, P., Amato, M., Kokkalis, A., Mottura, L., Serr, C., Larrey, E., Filippone, A., Fischer, A. 2001. "Helicopter Fuselage Drag Prediction: State of the art in Europe", AIAA paper 2001-0999. Proceedings of the 39th AIAA Aerospace Sciences Meeting & Exhibit. Reno, Nevada, January 08-11.

- Gomes, L.D., Crowther, W., Wood, N.J. (2006). "Towards a Practical Synthetic Jet Actuator for Industrial Scale Flow Control Applications", IUTAM Proceedings on Flow control and MEMS, Kluwer Academic Publishers.

- Gormont, R.E. 1975. "Some Important Practical Design Constraints Affecting Drag Reduction", Proceedings of the 31st Annual Forum of the American Helicopter Society. Special Report Presented by the AD HOC Committee on Rotorcraft Drag. Washington, D.C., May 14-15.

- Greenwell, D.I. 1997. "Large excrescences on transport aircraft: a cautionary tale", The Aeronautical Journal, Paper No. 2263, pp. 327-330.

- Harrington, R.D. 1954. "Reduction of Helicopter Parasite Drag", NACA TN 3234.

- Hassan, A.A., Domzaiski, D.B., JanakiRam, R.D., Srinivasan, G.R. 1998. "Prospects of Using Zero-Mass 'Synthetic' Jets for Improved Helicopter/Tiltrotor Aerodynamic Performance", Proceedings of the 54th Annual Forum of the American Helicopter Society, Washington, D.C., May 20-22.

- Hermans, C., Hakkaart, J., Panosetti, G., Preatoni, G., Mikulla, V., Chéry, F., Serr, C. 1997. "Overview of the NH90 Wind Tunnel Test Activities and the Benefits to the Helicopter Development", Proceedings of the 53rd Annual Forum of the American Helicopter Society. Virginia Beach, Virginia, April 29-May 1.

- Hoffman, J.A. 1975. "The Relationship between Rotorcraft Drag and Stability and Control", Proceedings of the 31st Annual Forum of the American Helicopter Society. Special Report Presented by the AD HOC Committee on Rotorcraft Drag. Washington, D.C., May 14-15.

- Keys, C., Wiesner, R. 1975. "Guidelines for Reducing Helicopter Parasite Drag", Proceedings of the 31st Annual Forum of the American Helicopter Society. Special Report Presented by the AD HOC Committee on Rotorcraft Drag. Washington, D.C., May 14-15.

- Koike, M., Nagayoshi, T., Hamamoto, M. 2004. "Research on Aerodynamic Drag Reduction by Vortex Generators", Mitsubishi Motors Technical Review, No.16.

- Leishman, J.G. 2006 (1). "Achieving the Ultimate Potential of the Helicopter: Thinking Forward, Looking Back", Proceedings of the 45th Cierva Memorial Lecture of the Royal Aeronautical Society, pp.24-27.

- Leishman, J.G. 2006 (2). "Principles of Helicopter Aerodynamics", Cambridge University Press, New York.

- Lowson, M.V. 1980. "Thoughts on an Efficient Helicopter", Westland Helicopters Limited, Research Memorandum No. 490, March.

- Martin, P.B., Tung, C., Hassan, A.A., Cerchie, D., Roth, J. 2005. "Active Flow Control Measurements and CFD on a Transport Helicopter Fuselage", Proceedings of the 61st Annual Forum of the American Helicopter Society, Grapevine, Texas, June 1-3.

- Mazzucchelli, C., Wilson, F.T. 1991. “The Achievement of the Aerodynamic Goals on the EH-101 Project through the ‘Single Site’ Concept”, Proceedings of the 17th European Rotorcraft Forum, Paper No. 91 - 06, September 24-26.

- Perry, F.J. 1979. “A Brief Introduction to the Flows Associated with the Helicopter Fuselage”, Westland Helicopter Limited, Aeronautical Technical Note GEN/018, October.

- Perry, F.J. 1987. “Aerodynamics of the Helicopter World Speed Record”, Proceedings of the 43rd Annual Forum of the American Helicopter Society, St. Louis, Missouri, May 18-20.

- Polz, G., Quentin, J. 1981. “Separated Flows around Helicopter Bodies”, Proceedings of the 6th European Rotorcraft and Powered Lift Aircraft Forum, Paper No. 48, Munich, Germany, September 8-11.

- Prouty, R.W., Amer, K.B. 1982. “The YAH-64 Empennage and Tail Rotor - A Technical History”, Proceedings of the 38th Annual Forum of the American Helicopter Society, Culver City, California, May 4-7.

- Roesch, P. 1980. “Aerodynamic Design of the Aerospatiale SA 365 N - Dauphin 2 Helicopter”, Proceedings of the 6th European Rotorcraft and Powered Lift Aircraft Forum, Paper No. 28, Bristol, England, September 16-19.

- Roesch, P., Vuillet, A. 1981. “New Designs for Improved Aerodynamic Stability on Recent Aerospatiale Helicopters”, Proceedings of the 37th Annual Forum of the American Helicopter Society, New Orleans, Louisiana, May 17-20.
- Sampatacos, E.P., Morger, K.M., Logan, A.H. 1983.”NOTAR - The Viable Alternative to a Tail Rotor”, AIAA Paper 83-2527, AIAA Aircraft Design, Systems and Technology Meeting, Ft. Worth, TX, October 17-19.

- Seddon, J. 1982. “Aerodynamics of the Helicopter Rear Fuselage Upsweep”, Proceedings of the 8th European Rotorcraft Forum, Paper No. 2.12, Aix-en-Provence, France, August 31-September 3.

- Seddon, J. 1983. “Further Studies in Helicopter Body Aerodynamics”, Proceedings of the 9th European Rotorcraft and Powered Lift Aircraft Forum, Paper No. 13, Stresa, Italy, September 13-15.

- Stepniewski, W.Z., Keys, C.N. 1984. “Rotary-Wing Aerodynamics”, Dover Publications, New York. Volume II.

- Stroub, R.H., Rabbott Jr., J.P. 1975. “Wasted Fuel - Another Reason for Drag Reduction”, Proceedings of the 31st Annual Forum of the American Helicopter Society. Special Report Presented by the AD HOC Committee on Rotorcraft Drag. Washington, D.C., May 14-15.

- Vuillet, A., Morelli, F. 1986. “New Aerodynamic Design of the Fenestron for Improved Performance”, Proceedings of the 12th European Rotorcraft Forum, Garmisch-Partenkirchen, Germany, September 22-25.

- Wiesner, W., Snyder, W.J. 1977. “Efficient Civil Helicopters: The Payoff of Directed Research”, Proceedings of the 33rd Annual Forum of the American Helicopter Society, Washington, D.C., May 9-11.

- Williams, R.M., Montana, P.S. 1975. “A Comprehensive Plan for Helicopter Drag Reduction”, Proceedings of the 31st Annual Forum of the American Helicopter Society. Special Report Presented by the AD HOC Committee on Rotorcraft Drag. Washington, D.C., May 14-15.

- Wilson, F.T., Ahmed, S.R. 1991. “Fuselage Aerodynamic Design Issues and Rotor/Fuselage Interactional Aerodynamics. Part 1: Practical Design Issues”, AGARD, Aerodynamics of Rotorcraft, N91-18048.

- www.cleansky.com

Table A.1. FDS program simulation data for middle CG position at SL

Simulation	Velocity [knots]	CG position [m]	Tail Plane Incidence[deg]	Altitude [ft]	Drag [N]	Lift [N]	Tail Lift [N]	Power [hp]	Aircraft Incidence[deg]	Fuel Flow$_T$ [lb/hr]
A4	80	-0.155	5	SL	4631.5	702.7	383.6	2523.3	0.459	1492.68
A0	80	-0.155	3	SL	4631.8	856.6	233.3	2525.5	0.597	1493.4
A8	80	-0.155	0	SL	4630.1	1059.5	9.5	2529.2	0.807	1494.63
AC	80	-0.155	-5	SL	4618.8	1449.4	-522.7	2540.1	1.325	1498.23
AG	80	-0.155	-10	SL	4608.7	1809.6	-1012.2	2549.7	1.802	1501.41
AK	80	-0.155	-15	SL	4597.9	2208.3	-1551.7	2560.1	2.329	1504.83
A5	100	-0.155	5	SL	7247.4	-856.7	406.1	2684.2	-1.472	1545.78
A1	100	-0.155	3	SL	7247.4	-503.8	183.5	2683.6	-1.255	1545.57
A9	100	-0.155	0	SL	7247.6	122.5	-212.2	2682.7	-0.871	1545.3
AD	100	-0.155	-5	SL	7248.7	1365.3	-1000.4	2681.8	-0.108	1545
AH	100	-0.155	-10	SL	7232.5	2107.2	-1726.3	2689.6	0.621	1547.55
AL	100	-0.155	-15	SL	7209.6	2865.6	-2569.8	2700.6	1.475	1551.21
A6	120	-0.155	5	SL	10448.9	-6023.3	113.4	3231.4	-3.846	1733.97
A2	120	-0.155	3	SL	10446.7	-5126.2	-252.4	3217.4	-3.453	1729.08
AA	120	-0.155	0	SL	10443.7	-3627.4	-869.4	3195.8	-2.793	1721.52
AE	120	-0.155	-5	SL	10441.3	-1262.7	-1857.5	3166.1	-1.751	1711.14
AI	120	-0.155	-10	SL	10442	863	-2855.4	3147.1	-0.73	1704.48
AM	120	-0.155	-15	SL	10424.1	2849.9	-4013.5	3138.7	0.476	1701.54
A7	140	-0.155	5	SL	14005.1	-14085.4	-727.4	4278.5	-6.082	2100.48
A3	140	-0.155	3	SL	14074.5	-12745.9	-1257.6	4248.4	-5.583	2089.92
AB	140	-0.155	0	SL	14178.1	-10777.2	-2046	4207.1	-4.848	2075.49
AF	140	-0.155	-5	SL	14221.4	-6966.5	-3210.3	4108.7	-3.56	2041.05
AJ	140	-0.155	-10	SL	14214	-2509.3	-4467.6	4002.9	-2.1	2004
AN	140	-0.155	-15	SL	14214.7	1486.6	-5839.3	3933.7	-0.609	1979.79

Table A.2. FDS program simulation data for forward CG position at SL

Simulation	Velocity [knots]	CG position [m]	Tail Plane Incidence[deg]	Altitude [ft]	Drag [N]	Lift [N]	Tail Lift [N]	Power [hp]	Aircraft Incidence[deg]	Fuel Flow$_T$ [lb/hr]
AS	80	0.075	5	SL	4646.6	-2253.4	92.2	2566.7	-2.102	1507.02
AO	80	0.075	3	SL	4646	-2073	-81.7	2568.6	-1.94	1507.65
AW	80	0.075	0	SL	4645	-1737.4	-405	2572.2	-1.639	1508.82
B0	80	0.075	-5	SL	4643.6	-1212.3	-910.3	2577.6	-1.17	1510.62
B4	80	0.075	-10	SL	4642.4	-666.3	-1434.9	2583.1	-0.682	1512.42
B8	80	0.075	-15	SL	4641.5	-153.2	-1927.3	2588.1	-0.224	1514.07
AT	100	0.075	5	SL	7259.2	-5133.5	-23.7	2780.1	-4.047	1578.24
AP	100	0.075	3	SL	7264.6	-4659.3	-337.3	2778.1	-3.747	1577.55
AX	100	0.075	0	SL	7261.9	-3889.5	-807.1	2773	-3.278	1575.81
B1	100	0.075	-5	SL	7258.4	-2712.1	-1528.9	2765.9	-2.56	1573.41
B5	100	0.075	-10	SL	7255.8	-1449.4	-2307.2	2759.4	-1.791	1571.19
B9	100	0.075	-15	SL	7254.3	-307.3	-3014.5	2754.3	-1.094	1569.45
AU	120	0.075	5	SL	10282.5	-10637.1	-583.2	3379	-6.048	1785.63
AQ	120	0.075	3	SL	10322.2	-9863.5	-1007.6	3369.5	-5.66	1782.33
AY	120	0.075	0	SL	10380.1	-8746.9	-1623.8	3356.5	-5.1	1777.77
B2	120	0.075	-5	SL	10460.1	-6916.6	-2594.7	3334.5	-4.2	1770.06
B6	120	0.075	-10	SL	10451.7	-4250.1	-3666.8	3286.3	-3.036	1753.2
BA	120	0.075	-15	SL	10448	-2442.1	-4406.3	3257.5	-2.244	1743.12
AV	140	0.075	5	SL	13767.5	-19052.7	-1872.8	4538	-7.874	2191.68
AR	140	0.075	3	SL	13821.4	-17949.3	-2289.3	4504.4	-7.469	2179.59
AZ	140	0.075	0	SL	13903.7	-16287	-2923.4	4456.1	-6.857	2162.64
B3	140	0.075	-5	SL	14064.7	-13109.6	-4157.9	4371.4	-5.682	2132.97
B7	140	0.075	-10	SL	14235.7	-9417.7	-5573.9	4281.8	-4.328	2101.62
BB	140	0.075	-15	SL	14228.7	-7343.3	-6130.4	4218.6	-3.656	2079.51

Table A.3. FDS program simulation data for rearward CG position at SL

Simulation	Velocity [knots]	CG position [m]	Tail Plane Incidence[deg]	Altitude [ft]	Drag [N]	Lift [N]	Tail Lift [N]	Power [hp]	Aircraft Incidence[deg]	Fuel Flow$_T$ [lb/hr]
BG	80	-0.385	5	SL	4574.5	2722.4	712	2515	3.05	1489.95
BC	80	-0.385	3	SL	4572.1	2818.7	530.7	2519.7	3.219	1491.51
BK	80	-0.385	0	SL	4568.8	2950.3	283.1	2526.1	3.45	1493.61
BO	80	-0.385	-5	SL	4563.1	3176.7	-141.9	2536.7	3.847	1497.12
BS	80	-0.385	-10	SL	4555.5	3468.3	-687.9	2550.1	4.359	1501.53
BW	80	-0.385	-15	SL	4548.5	3734.6	-1185.2	2561.7	4.826	1505.37
BH	100	-0.385	5	SL	7212.3	2523.3	812.4	2638	1.093	1530.54
BD	100	-0.385	3	SL	7205.8	2747.5	559.8	2642.1	1.345	1531.89
BL	100	-0.385	0	SL	7197	3052.2	216.7	2647.9	1.688	1533.81
BP	100	-0.385	-5	SL	7178.3	3691.6	-502.8	2659.5	2.408	1537.62
BT	100	-0.385	-10	SL	7157.9	4381.8	-1278.6	2671.8	3.185	1541.7
BX	100	-0.385	-15	SL	7137.6	5059.3	-2039.3	2683.6	3.947	1545.57
BI	120	-0.385	5	SL	10433.6	-157.5	691.2	3086.5	-1.271	1683.27
BE	120	-0.385	3	SL	10434.4	429.9	377.9	3084.1	-0.959	1682.43
BM	120	-0.385	0	SL	10435.7	1375.1	-128	3080.9	-0.458	1681.32
BQ	120	-0.385	-5	SL	10410.1	3112	-1211.4	3081	0.683	1681.35
BU	120	-0.385	-10	SL	10367.5	4496.7	-2197.1	3085.8	1.765	1683.03
BY	120	-0.385	-15	SL	10321.7	5973.5	-3252.2	3092.3	2.92	1685.31
BJ	140	-0.385	5	SL	14215.7	-8190.8	154.6	4044.2	-3.986	2018.46
BF	140	-0.385	3	SL	14212	-6598.6	-287.9	4005.6	-3.464	2004.96
BN	140	-0.385	0	SL	14207.9	-3959.8	-1038.3	3948	-2.596	1984.8
BR	140	-0.385	-5	SL	14207.7	-25	-2308.8	3880.9	-1.197	1961.31
BV	140	-0.385	-10	SL	14202.5	3280.1	-3552	3842.9	0.133	1948.02
BZ	140	-0.385	-15	SL	14111.5	6169.1	-4901.5	3823.7	1.793	1941.3

Table A.4. FDS program simulation data for middle CG position at 4000ft

Simulation	Velocity [knots]	CG position [m]	Tail Plane Incidence[deg]	Altitude [ft]	Drag [N]	Lift [N]	Tail Lift [N]	Power [hp]	Aircraft Incidence[deg]	Fuel Flow$_T$ [lb/hr]
C4	80	-0.155	5	4000	4109.3	504.1	328.4	2725.1	0.874	1491.03
C0	80	-0.155	3	4000	4109.4	629.3	194.1	2727.7	0.996	1491.96
C8	80	-0.155	0	4000	4109.7	818.9	-9.3	2731.4	1.181	1493.31
CC	80	-0.155	-5	4000	4101.6	1156.8	-492.3	2743.7	1.642	1497.72
CG	80	-0.155	-10	4000	4093.1	1447.1	-929	2755	2.063	1501.8
CK	80	-0.155	-15	4000	4083.8	1775.5	-1420.7	2767.2	2.537	1506.18
C5	100	-0.155	5	4000	6434.2	-231.9	412.9	2807	-0.851	1520.52
C1	100	-0.155	3	4000	6434.2	53.8	212.2	2807.6	-0.659	1520.73
C9	100	-0.155	0	4000	6434.5	534	-125.4	2808.6	-0.337	1521.09
CD	100	-0.155	-5	4000	6431.6	1502.8	-839.1	2811.9	0.353	1522.29
CH	100	-0.155	-10	4000	6412	2163.2	-1474.9	2820.3	1.01	1525.32
CL	100	-0.155	-15	4000	6394.2	2766.6	-2227.6	2834.8	1.757	1530.51
C6	120	-0.155	5	4000	9275.5	-3888.3	244.1	3284.2	-2.937	1689.45
C2	120	-0.155	3	4000	9274.2	-3285.7	-36.8	3276.1	-2.645	1686.63
CA	120	-0.155	0	4000	9272.3	-2079.2	-602.8	3260.7	-2.061	1681.23
CE	120	-0.155	-5	4000	9271	-139.7	-1522.5	3239	-1.121	1673.64
CI	120	-0.155	-10	4000	9271.8	1594.4	-2405.6	3224.9	-0.236	1668.72
CM	120	-0.155	-15	4000	9241.8	2975.8	-3454.6	3228.1	0.868	1669.83
C7	140	-0.155	5	4000	12534.8	-10695.6	-339.9	4291.7	-5.132	2046
C3	140	-0.155	3	4000	12591.6	-9607.2	-827.6	4269.4	-4.683	2037.99
CB	140	-0.155	0	4000	12635.2	-7704.1	-1543	4221.5	-3.953	2020.74
CF	140	-0.155	-5	4000	12625.6	-4324.5	-2608.5	4127.2	-2.739	1986.78
CJ	140	-0.155	-10	4000	12621	-832.8	-3746.5	4044.3	-1.477	1956.96
CN	140	-0.155	-15	4000	12622.2	2500.4	-5066.5	3988.7	-0.091	1936.92

Table A.5. FDS program simulation data for forward CG position at 4000ft

Simulation	Velocity [knots]	CG position [m]	Tail Plane Incidence[deg]	Altitude [ft]	Drag [N]	Lift [N]	Tail Lift [N]	Power [hp]	Aircraft Incidence[deg]	Fuel Flow$_T$ [lb/hr]
CS	80	0.075	5	4000	4128	-2170.6	-19.9	2775.6	-1.622	1509.21
CO	80	0.075	3	4000	4127.3	-2005.4	-195.2	2778.3	-1.46	1510.2
CW	80	0.075	0	4000	4126.2	-1756.5	-459.5	2782.6	-1.217	1511.73
D0	80	0.075	-5	4000	4124.8	-1374.1	-865.1	2788.9	-0.843	1514.01
D4	80	0.075	-10	4000	4123.2	-935.5	-1328.8	2795.9	-0.416	1516.53
D8	80	0.075	-15	4000	4122	-559.9	-1725.4	2801.5	-0.05	1518.54
CT	100	0.075	5	4000	6453.6	-4193.2	23.6	2906.5	-3.438	1556.34
CP	100	0.075	3	4000	6451.9	-3793.5	-248.7	2904.9	-3.171	1555.77
CX	100	0.075	0	4000	6449.5	-3169.1	-674.5	2902.7	-2.755	1554.96
D1	100	0.075	-5	4000	6446.3	-2208	-1331.8	2899.7	-2.113	1553.88
D5	100	0.075	-10	4000	6443.7	-1185.8	-2033	2897.2	-1.431	1552.98
D9	100	0.075	-15	4000	6442.1	-250.5	-2676.3	2895.3	-0.807	1552.32
CU	120	0.075	5	4000	9182	-8549.8	-365.5	3448.1	-5.286	1746.84
CQ	120	0.075	3	4000	9214.2	-7919.2	-752.9	3442.5	-4.938	1744.86
CY	120	0.075	0	4000	9262.6	-6985.5	-1328.6	3434.7	-4.422	1742.13
D2	120	0.075	-5	4000	9288.4	-5287.4	-2192.7	3409.6	-3.565	1733.34
D6	120	0.075	-10	4000	9281.5	-3169.3	-3160	3373.9	-2.548	1720.86
DA	120	0.075	-15	4000	9278.2	-1582.5	-3894	3349.8	-1.785	1712.43
CV	140	0.075	5	4000	12312.6	-15345.5	-1375.3	4552.5	-6.983	2141.46
CR	140	0.075	3	4000	12359.3	-14390.1	-1785.3	4525.4	-6.595	2130.9
CZ	140	0.075	0	4000	12425.6	-13049.6	-2365.1	4488.7	-6.049	2116.92
D3	140	0.075	-5	4000	12555.4	-10485.3	-3489.6	4423.8	-5.001	2093.58
D7	140	0.075	-10	4000	12640.8	-7150.8	-4755.5	4330.8	-3.718	2060.1
DB	140	0.075	-15	4000	12633.9	-5086.1	-5397.1	4266.2	-2.981	2036.82

Table A.6. FDS program simulation data for rearward CG position at 4000ft

Simulation	Velocity [knots]	CG position [m]	Tail Plane Incidence[deg]	Altitude [ft]	Drag [N]	Lift [N]	Tail Lift [N]	Power [hp]	Aircraft Incidence[deg]	Fuel Flow$_T$ [lb/hr]
DG	80	-0.385	5	4000	4054.4	2477.9	642.5	2711.9	3.466	1486.29
DC	80	-0.385	3	4000	4052.1	2582.1	484.8	2716.5	3.616	1487.94
DK	80	-0.385	0	4000	4049.1	2726.5	267	2722.7	3.823	1490.16
DO	80	-0.385	-5	4000	4044.1	2966.3	-93.5	2732.7	4.166	1493.76
DS	80	-0.385	-10	4000	4038.4	3210.7	-584.7	2747.8	4.623	1499.19
DW	80	-0.385	-15	4000	4031.6	3417.6	-1029.2	2761.3	5.036	1504.05
DH	100	-0.385	5	4000	6386.7	2741.5	808.2	2762.6	1.73	1504.53
DD	100	-0.385	3	4000	6381.5	2926.5	568.1	2768.2	1.964	1506.54
DL	100	-0.385	0	4000	6374.8	3165.4	258.3	2775.4	2.267	1509.15
DP	100	-0.385	-5	4000	6361.1	3646.7	-365.1	2789.4	2.877	1514.19
DT	100	-0.385	-10	4000	6345.2	4196.2	-1075.5	2805	3.573	1519.8
DX	100	-0.385	-15	4000	6329.8	4723.1	-1755.4	2819.6	4.24	1525.05
DI	120	-0.385	5	4000	9263.8	1329.9	759.7	3144.1	-0.393	1640.43
DE	120	-0.385	3	4000	9264.6	1791.2	474.3	3144.1	-0.117	1640.43
DM	120	-0.385	0	4000	9254.1	2350	52.4	3147.3	0.319	1641.54
DQ	120	-0.385	-5	4000	9219	3510.5	-910.2	3157.9	1.341	1645.26
DU	120	-0.385	-10	4000	9185.4	4615.4	-1828.5	3168.3	2.314	1648.89
DY	120	-0.385	-15	4000	9150.4	5757.2	-2778.7	3179.5	3.319	1652.82
DJ	140	-0.385	5	4000	12616.6	-4332.4	426.3	4015.1	-2.771	1946.43
DF	140	-0.385	3	4000	12615.1	-3283.2	83.2	3991.8	-2.391	1938.06
DN	140	-0.385	0	4000	12613.5	-1261.9	-587.9	3950.6	-1.656	1923.21
DR	140	-0.385	-5	4000	12615.3	1840.9	-1809.8	3905.2	-0.38	1906.86
DV	140	-0.385	-10	4000	12573.9	4060.2	-2926.4	3888.6	0.876	1901.01
DZ	140	-0.385	-15	4000	12504.5	6279.1	-4157.7	3881.3	2.311	1898.46

Table B.1. Engine Manufacture (Rolls-Royce RTM322-02/8 MK200) table of fuel flow per engine

0	100	200	300	400	500	600	700	800	900	1000	1100	1200	1300	Power(hp)/Altitude(ft)
212	212	282	331	368	402	435	468	499	532	564	599	633	667	**-2000**
213	**213**	**273**	**320**	**356**	**392**	**422**	**453**	**484**	**517**	**551**	**586**	**621**	**656**	**0**
207	207	264	306	344	372	402	435	471	505	539	575	610	645	**2000**
190	**190**	**255**	**293**	**337**	**360**	**390**	**425**	**459**	**494**	**530**	**565**	**600**	**635**	**4000**
187	187	247	283	322	346	380	415	450	485	520	555	590	626	**6000**
184	184	238	275	306	336	372	406	441	476	511	546	582	619	**8000**
181	181	229	268	293	328	363	398	433	467	503	538	575	615	**10000**
178	178	219	257	284	320	355	390	425	459	496	532	573	615	**12000**
174	174	210	243	276	312	348	382	416	452	489	529	571	615	**14000**
166	166	204	232	270	305	340	374	410	446	485	527	571	619	**16000**
159	159	197	227	264	299	333	368	404	442	483	526	575	0	**18000**
151	151	191	223	259	294	328	364	400	440	482	531	0	0	**20000**
1400	**1500**	**1600**	**1700**	**1800**	**1900**	**2000**	**2100**	**2200**	**2300**	**2400**	**2500**	**2600**	**2700**	**Power(hp)/Altitude(ft)**
703	738	773	809	845	883	922	964	1007	1052	1097	1139	1180	0	**-2000**
691	**726**	**762**	**798**	**836**	**876**	**919**	**963**	**1008**	**1052**	**1094**	**1137**	**0**	**0**	**0**
680	716	752	790	831	875	919	965	1007	1051	0	0	0	0	**2000**
671	**707**	**746**	**787**	**831**	**876**	**921**	**964**	**0**	**0**	**0**	**0**	**0**	**0**	**4000**
663	702	744	788	833	877	922	0	0	0	0	0	0	0	**6000**
658	701	745	790	834	0	0	0	0	0	0	0	0	0	**8000**
658	702	747	793	0	0	0	0	0	0	0	0	0	0	**10000**
659	704	0	0	0	0	0	0	0	0	0	0	0	0	**12000**
662	0	0	0	0	0	0	0	0	0	0	0	0	0	**14000**
0	0	0	0	0	0	0	0	0	0	0	0	0	0	**16000**
0	0	0	0	0	0	0	0	0	0	0	0	0	0	**18000**
0	0	0	0	0	0	0	0	0	0	0	0	0	0	**20000**